

Effect of the Hadron Hose on MINOS Physics

Liz Buckley-Geer, Sacha Kopp, Mikhail Kostin, Mark Messier
Fermi National Accelerator Laboratory, Harvard University,
University of Texas

Abstract

The Hadron Hose increases the flux of ν_μ 's reaching the far MINOS detector, while reducing distortions in the far/near ratio which could cause poorer resolutions in oscillation fits or lead to a less precise capability of the experiment to distinguish standard oscillations from ν_μ disappearance caused by other phenomena. In this note, we study the effect of reducing such distortions on the disappearance measurement of charged current events and on MINOS' ability to distinguish between $\nu_\mu - \nu_\tau$ oscillations and alternative hypotheses. Finally, we study the effect of the increased ν_e flux from the hose on ν_e appearance searches.

1 Introduction

The MINOS experiment will be the premier long baseline neutrino physics experiment for the next decade. Following the indications from Super Kamiokande and K2K, from which we may be tempted to believe strongly that some effect causes ν_μ disappearance, MINOS has the unique possibility to map out the nature of this phenomenon. Super Kamiokande, which suffers in L/E resolution, cannot give an accurate determination of the oscillation parameters, and cannot exclude other models[9, 10] which could result in ν_μ disappearance. K2K, furthermore, will never have the statistics to perform such detailed measurements, nor to look for possible sub-dominant oscillation modes. It is therefore critical that MINOS be able to capitalize on its unique position as a precision neutrino physics experiment by (1) quantitatively demonstrating that the disappearance effect follows the expected oscillation or other model's spectral shape and (2) searching for other, subdominant modes.

The hadron hose [1, 2] improves the physics capabilities of the MINOS experiment because it extends the focusing of the two horn system for NuMI. For the pions which are overfocused or underfocused by the horns, the resulting neutrino flux is sensitive to the details of particle production in the target. Our ability to predict the spectrum of neutrinos, particularly in the high energy tail, is improved by the hadronic hose which randomizes the correlations left by the horns between production p_T and angle of the pion when it decays. As well, the hose increases the flux of low energy neutrinos which originate from wide angle soft pions which would interact in the decay pipe walls without the hose focusing. Finally, the hadron hose also broadens and smooths the neutrino energy spectrum in both the near and far detectors. This is attractive in an experiment in which we are trying to detect sharp deviations in

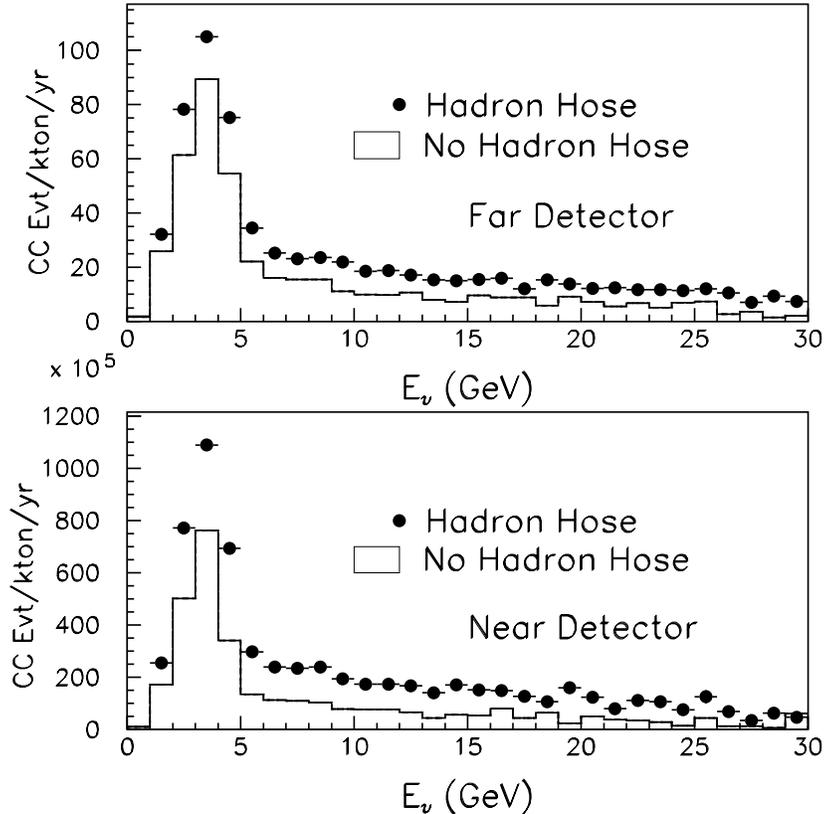


Figure 1: The neutrino energy spectrum expected in the near and far MINOS detectors, with and without the hadron hose. Shown are the results for one kt-yr. exposure (taken from Ref [3]).

the ν_μ energy spectrum. An example of the neutrino spectra expected in the near and far detectors, with and without the hadron hose, is shown in Figure 1.

Finally, it should be noted that the hadron hose will lessen the experiment's sensitivity to running conditions, such as horn misalignments, primary beam targeting, *etc.* This will be extremely important, especially in the beginning of the running period, where many systems will be checked and fine-tuned. Because the hose minimizes the spectral distortions from several such potential problems, we can hope that we will lose less time during the commissioning period and that physics-quality data taking can begin sooner. Such statements are difficult to quantify *a priori*, of course, but it would be nice to have this extra insurance policy. One example of how the hose makes MINOS less sensitive to such beam conditions is shown in Figure 2, where a 1 or 2 mm misalignment of the horn is shown to cause a much smaller relative variation in the neutrino energy spectrum. These kinds of beam conditions will not be considered further in this note, but are an important argument in favor of the hadron hose as an 'insurance policy' for MINOS.

The main issue addressed by this note is how the hadron hose lessens the experiment's sensitivity to one important beam systematic, namely the cross sections for particle production in the target. Detailed studies of the neutrino spectra in the near and far detectors with

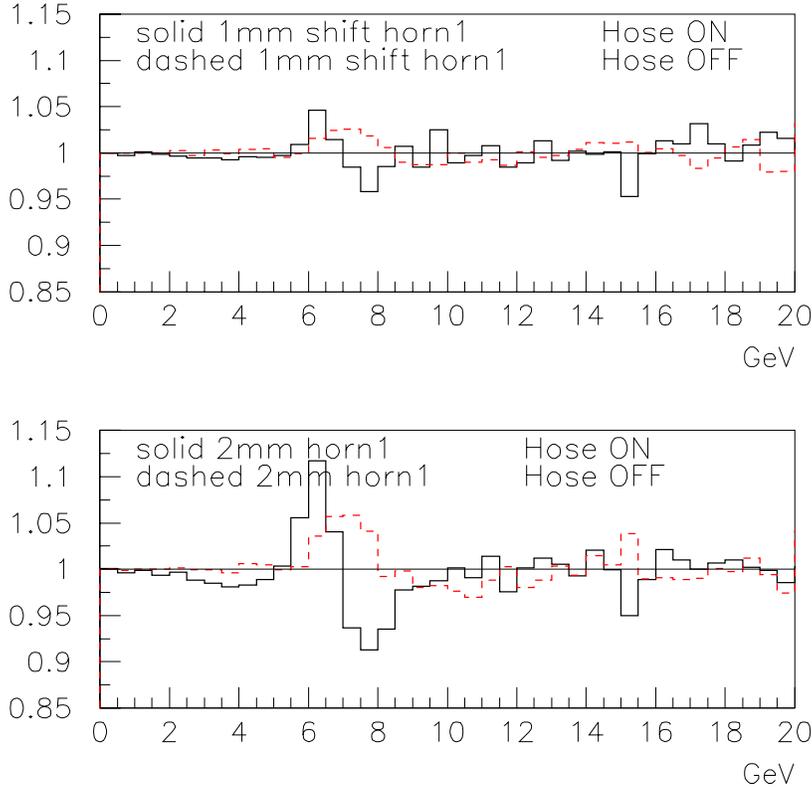


Figure 2: The “double-ratio” of Far/Near (spectrum in the far detector divided by the spectrum in the near detector) for the case of a displacement of a magnetic horn, relative to the nominal F/N ratio. Shown are the relative distortions for a 1 mm and a 2 mm horn displacement, with and without the hose. The hose results in a factor of two less spectral distortion (PLEASE NOTE THAT THE CAPTIONS WITHIN THE FIGURES ARE REVERSED! Solid = no hose, Dashed = hose).

and without the hose, and in particular studies of our sensitivity to different particle production models, has been presented in a separate NuMI note [3]. In this note, we summarize the impact of these uncertainties on MINOS physics. If beam systematics are not taken into account, they manifest themselves as distortions in the near/far spectra which could affect oscillation fits. Alternatively, these distortions can be taken as systematic uncertainties. We investigate the ramifications of both scenarios.

In brief, the systematic distortions from the beam can (1) produce false oscillation signals even when no oscillations are present, (2) wash out oscillations on the edge of MINOS’ sensitivity, (3) produce oscillation fits with poor χ^2 , reducing the scientific community’s confidence in an oscillation signal, and (4) reduce the experiment’s sensitivity to “new physics.” As we show in this note, all of these effects are improved with the addition of the hadronic hose. Finally, we consider the fact that the hose does increase the ν_e contamination in the beam by focussing μ ’s in the decay pipe. We investigate the effect this increase has on searches for $\nu_\mu - \nu_e$ oscillations.

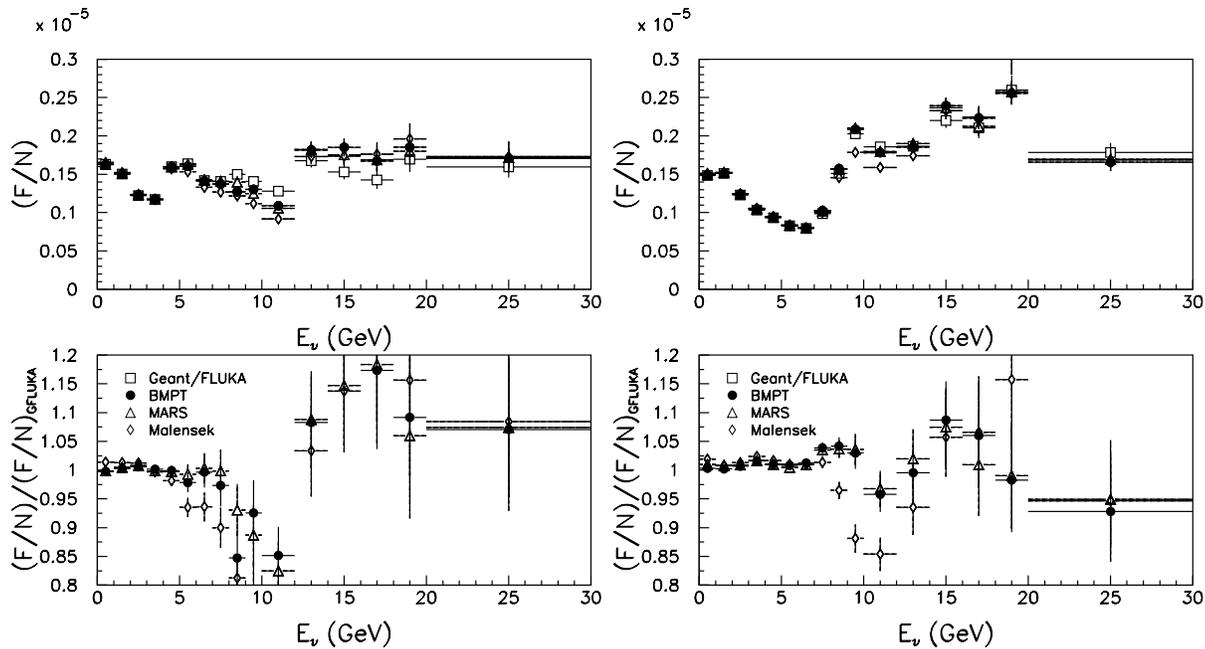


Figure 3: The far over near ratio \mathcal{R}_{FN} that would be used to extrapolate the near detector spectrum to the far detector. The far-near ratio is calculated for each of the particle production models (top plots), and then compared to the Geant/FLUKA model (lower plots). The far-near ratio is calculated for the PH2LE (left) and PH2ME (right) beams for the no-hose scenario. In the high energy tail, model variations approach 20%, while in the low energy peak variations are typically 2%.

2 Near-Far Extrapolation

The various models of particle production in the target actually predict variations in the neutrino flux and the spectral shape which approach 15-20%. However, these beam variations are, to first order, corrected by the near detector, because it measures the flux directly. As described in a separate NuMI note[3], the residual systematics from the beam are second order and come from our knowledge of how to extrapolate the measured near spectrum to the far detector:

$$N_{\text{far}}^i = N_{\text{near}}^i \times \mathcal{R}_{FN}^i$$

where N_{near}^i is the flux observed in the near detector in a particular energy bin i , N_{far}^i is the expected flux in the far detector, and \mathcal{R}_{FN}^i is the extrapolation factor which must be calculated from Monte Carlo. For the hose, this extrapolation factor is more nearly the pion lifetime [1], so that systematic uncertainties from particle production in the target or propagation through the beam optics which could affect \mathcal{R}_{FN}^i have a smaller effect.

Figure 3 shows the expected far-over-near ratio \mathcal{R}_{FN} calculated with no hadronic hose, for both the PH2LE and PH2ME beams. The far-over-near ratio is calculated for several models of particle production in the NuMI target [4, 5, 6, 7], which our calculations show to be the dominant systematic uncertainty in the beam extrapolation. Also shown is the variation of the models with respect to the Geant/FLUKA Monte Carlo (lower plots). Figure 4 shows \mathcal{R}_{FN} with the hose. As can be seen, the hose extends the focussing of the horns into the high

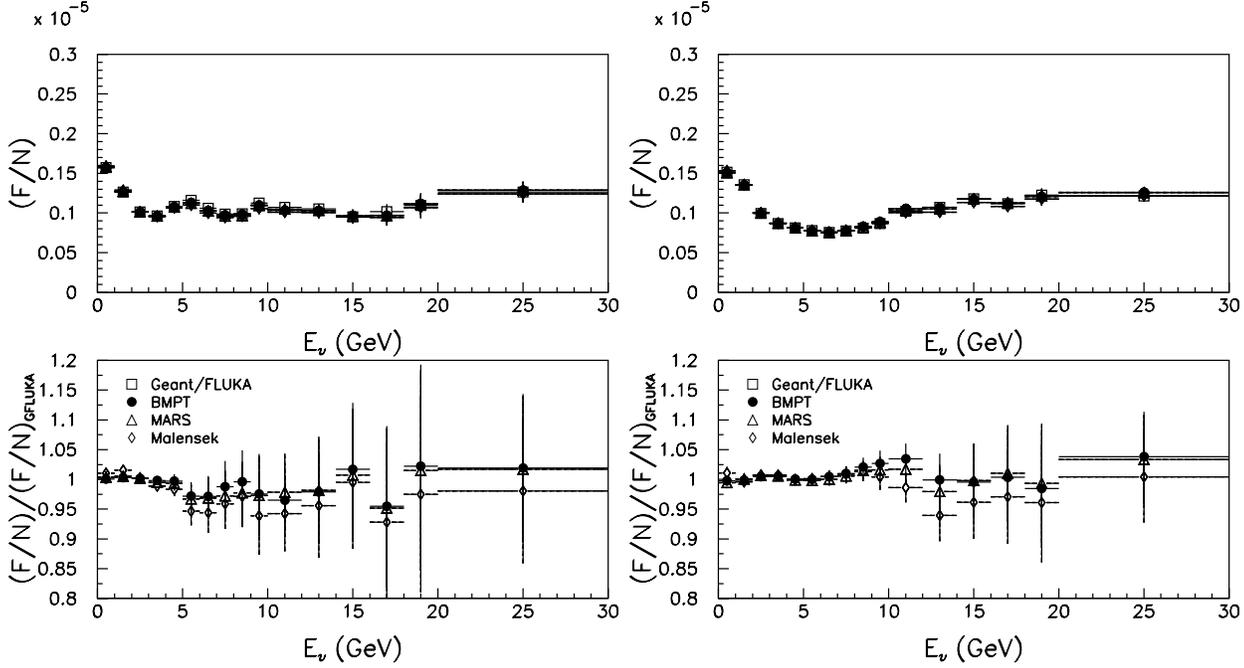


Figure 4: The far over near ratio \mathcal{R}_{FN} that would be used to extrapolate the near detector spectrum to the far detector. The far-near ratio is calculated for each of the particle production models (top plots), and then compared to the Geant/FLUKA model (lower plots). The far-near ratio is calculated for the PH2LE (left) and PH2ME (right) beams with the hadronic hose included.

energy tail, and reduces the $\sim 15\%$ variations in the tail due to various models of particle production in the target. Even in the region $E_\nu < 6$ GeV, the hose helps reduce the $\sim 1 - 2\%$ variations in the spectra.

It must be noted that the near MINOS detector actually serves two functions: (1) measure the neutrino spectrum produced by the NuMI beam, and (2) measure poorly known properties of neutrino cross sections at the very low energies ($\sim 1 - 5$ GeV) being probed by MINOS. Just as the NuMI spectrum can affect the rates observed in the far detector, so can the cross sections, y distributions, or properties of the hadronic recoil in CC interactions affect the spectrum reconstructed in the far detector. If the beam variations are under sufficiently poor control, then the near detector can do a less complete job of measuring these neutrino detection properties. While it is true that the experiment is only sensitive to the “product” of these two effects, it is also true that there is an equivalent extrapolation between the near and far detectors that must be understood. Thus, minimizing the beam variations with the hadronic hose can help better understand the issues of neutrino interactions and detection in the near and far detectors.

3 Method of this Note

In this note, we draw on the spectra calculated in [3] to generate MINOS “experiments”, which consist of near and far detector spectra scaled to the number of kt-years. We fit the far “experiments” generated under various models to “templates.” The templates consist of the near detector experiment’s spectrum extrapolated to the far detector using the factor \mathcal{R}_{FN} . The near and far experiments are always generated under the same conditions (hose on/off, choice of hadron production model). However, the factor \mathcal{R}_{FN} is always calculated using the Geant/FLUKA model.

Except in the ν_e appearance study, charged current muon events are used exclusively in this analysis. The reconstructed neutrino energy is obtained by adding the muon momentum, measured from its curvature in the magnetic field, with the hadronic shower energy measured in the MINOS calorimeter. We have smeared the energies by the nominal muon momentum and hadron energy resolution from the MINOS TDR. The y distribution is simply generated according to DIS. Neutrino reconstruction and trigger efficiencies [8] are applied to each event. If oscillations are introduced into an experiment, then a disappearance probability for the particular Δm^2 and $\sin^2(2\theta)$ is applied to each neutrino drawn from the spectra. A simple χ^2 test is performed to find the template which best matches the far detector spectrum over the first 20 GeV of the neutrino spectrum.

In this note, we investigate the effect of the beam systematics/distortions in two ways:

- First, we directly fit our far detector “experiments” to the extrapolated fluxes. Because the experiments were generated with different particle production models than what was used to calculate \mathcal{R}_{FN} , we potentially fit the data to the “wrong” templates.
- In the second test, we used the spread of the various particle production models’ predictions for \mathcal{R}_{FN} as a measure of the “systematic error” from the beam. This systematic error was then incorporated in the χ^2 fit of the observed far data to the extrapolated templates, as follows:

$$\chi^2 = \sum_{i=1}^{20\text{GeV}} \frac{(obs_i - expect_i)^2}{\sigma^2} \quad (1)$$

where $\sigma^2 \rightarrow \sigma_{stat}^2 + \sigma_{beam}^2$ and σ_{beam} is the spread from the various models. As with the first kind of test, the model used to generate the experiment was allowed to ‘float’ while the model used to calculate \mathcal{R}_{FN} was fixed to be the Geant/FLUKA model.

Most of the simulations performed in this note will correspond to 10 kilton-years of data, which is equivalent to 2 years of running with the nominal MINOS far detector. However, it is clear that should an oscillation-type effect be observed, further running will be warranted to explore the nature of the disappearance phenomenon. Therefore, we have in some cases run our simulations for 20 or 30 kt-yrs to demonstrate the long-term impact of systematic uncertainties on parameter measurements or discovery potentials.

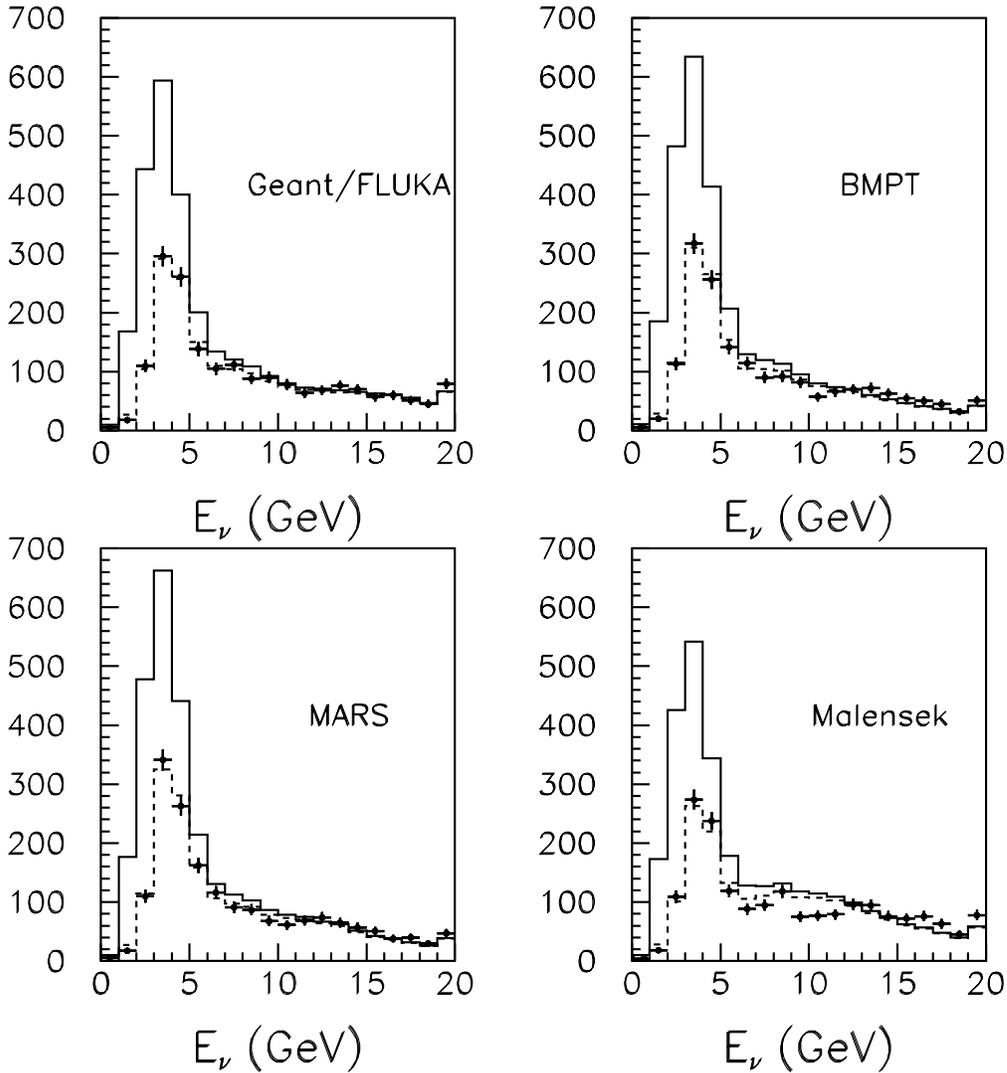


Figure 5: Simulation of a MINOS experiment of 10 kt-yr. exposure in the PH2LE beam with no hadronic hose. The data were generated with $\Delta m^2 = 0.003 \text{eV}^2$ and $\sin^2(2\theta) = 1.0$. The solid histogram is the expectation for no oscillations, and the dashed is the expectation for oscillations (both calculated using Geant/FLUKA[4] for \mathcal{R}_{FN}). When a different model is used to generate the experiment, distortions relative to the expectation are evident.

4 CC Energy Measurement

This section describes what affects the model distortions/uncertainties can have on the neutrino energy spectrum measurement performed on CC events. The measurement of this spectrum will be one of the most important methods used to confirm the $\nu_\mu - \nu_\tau$ or some other model of ν_μ disappearance such as neutrino decay, sterile neutrinos, or extra dimensions. An example of four MINOS “experiments” created with the Geant/FLUKA, BMPT, MARS, or Malensek models are shown in Figure 5. In each, a 10 kt-year exposure was simulated in the PH2LE beam with no Hadron Hose focusing. The far data was generated with $\sin^2(2\theta) = 1.0$, $\Delta m^2 = 0.003 \text{eV}^2$. The observed far detector spectrum (shown in dots) is shown along with the extrapolated expectations with no oscillations (solid histogram) and with $\Delta m^2 = .003 \text{eV}^2$ (dashed histogram). Figure 6 shows the same thing, but with the

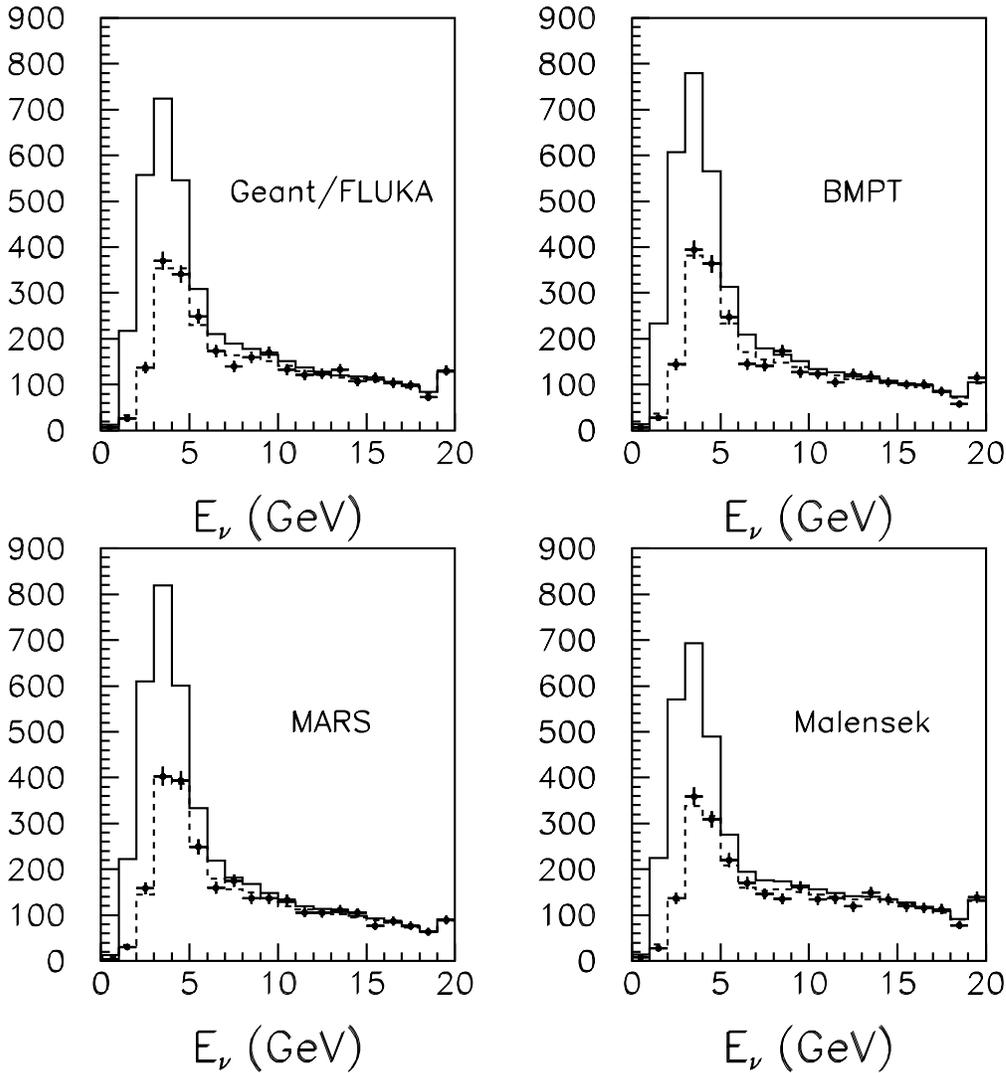


Figure 6: Simulation of a MINOS experiment of 10 kt-yr. exposure in the PH2LE beam with hadronic hose. The data were generated with $\Delta m^2 = 0.003\text{eV}^2$ and $\sin^2(2\theta) = 1.0$. The solid histogram is the expectation for no oscillations, and the dashed is the expectation for oscillations.

addition of hose focusing. Without the hose, distortions are evident when models used to generate the experiment are different from the Geant/FLUKA model used to calculate \mathcal{R}_{FN} .

The best oscillation fits to the data in Figure 5 give $\chi^2 = 20, 28, 23,$ and $48,$ respectively, for the four models. There are 18 degrees of freedom in the fit (20 bins of energy minus two parameters in the oscillation fit). With the hose on, the χ^2 's are 16, 16, 15, and 16. The disagreement without the hose comes mostly in the high energy tail of the neutrino energy spectrum, which is expected since it is in this region where the models disagree most.

As is clear from comparing the two figures, the hose yields approximately 30% more events in the peak (0-6 GeV) of the distributions for the PH2LE beam (2350 *vs.* 1810 events expected in the two Geant/FLUKA experiments shown in Figure 5 and 6). Thus, while some oscillation fits shown later in this section are improved with the hose as a result of distortions being removed from the extrapolation, at low energy the oscillation fits benefit from the increased statistics.

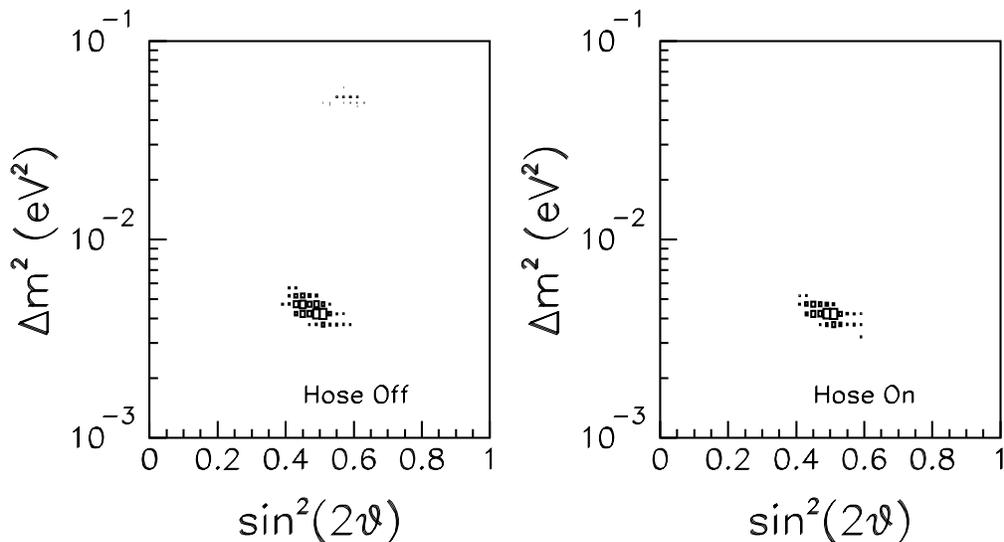


Figure 7: Simulation of 1000 MINOS experiments of 10 kt-yr. exposure in the PH2LE beam. The data were generated with $\Delta m^2 = 0.005\text{eV}^2$ and $\sin^2(2\theta) = 0.5$ and the hadron production model of Malensek[7]. The data in each experiment, however, were fitted to templates created using the Geant/FLUKA model to calculate \mathcal{R}_{FN} . With the hose off, the systematic distortions result in poorer fit resolutions and, for some experiments, false minima in the χ^2 .

4.1 How Unknown Distortions Affect Fits

First we allow the data to be distorted by the various models, as described above, and investigate what happens to oscillation fits when the distortions are not accounted for.

In some regions of parameter space distortions in the neutrino energy spectrum can skew the fitted results expected in MINOS. Figure 7 shows the best fit values of Δm^2 and $\sin^2(2\theta)$ from 1000 MINOS experiments which were generated with $\Delta m^2 = 0.005\text{eV}^2$ and $\sin^2(2\theta) = 0.5$. Even ignoring the poor fits at anomalously high Δm^2 , the resolution in both Δm^2 and $\sin^2(2\theta)$ are 20 % better when the focussing of the hose is present as compared to the no-hose case. This improvement comes about because the oscillation minimum for this Δm^2 occurs at $E_\nu \sim 5$ GeV, which approaches the tail of the low-energy beam where the horn focussing is absent.

In other regions of parameter space, the oscillation minimum in the neutrino energy spectrum is far away from the high energy tail where spectral distortions from the beam are largest. In such scenarios, the fitted parameters are negligibly changed, even with the hose off. In these cases, the systematic distortions from the beam show themselves as extremely poor values of χ^2 of the best fit, as shown in Figure 8. Without the hose, MINOS's data could have a $\text{Prob}(\chi^2) < 10\%$ in approximately 10, 54, 43, or 97% of experiments (depending on which model – Geant/FLUKA, BMPT, MARS, or Malensk, respectively – is chosen to represent the distortions). With the hose, this always happens in just 10% of experiments. It will be extremely difficult to claim an oscillation signal based on the disagreement of our data with expectations in one region of the E_ν plot when the rest of the plot where oscillations are not present does not agree with expectations. Such a poor fit will decrease the community's acceptance of any eventual oscillation signal claimed by the experiment.

We investigated whether or not the distortions are large enough to generate false oscillation signals. even in the absence of real oscillations. We simulated 1000 MINOS experiments

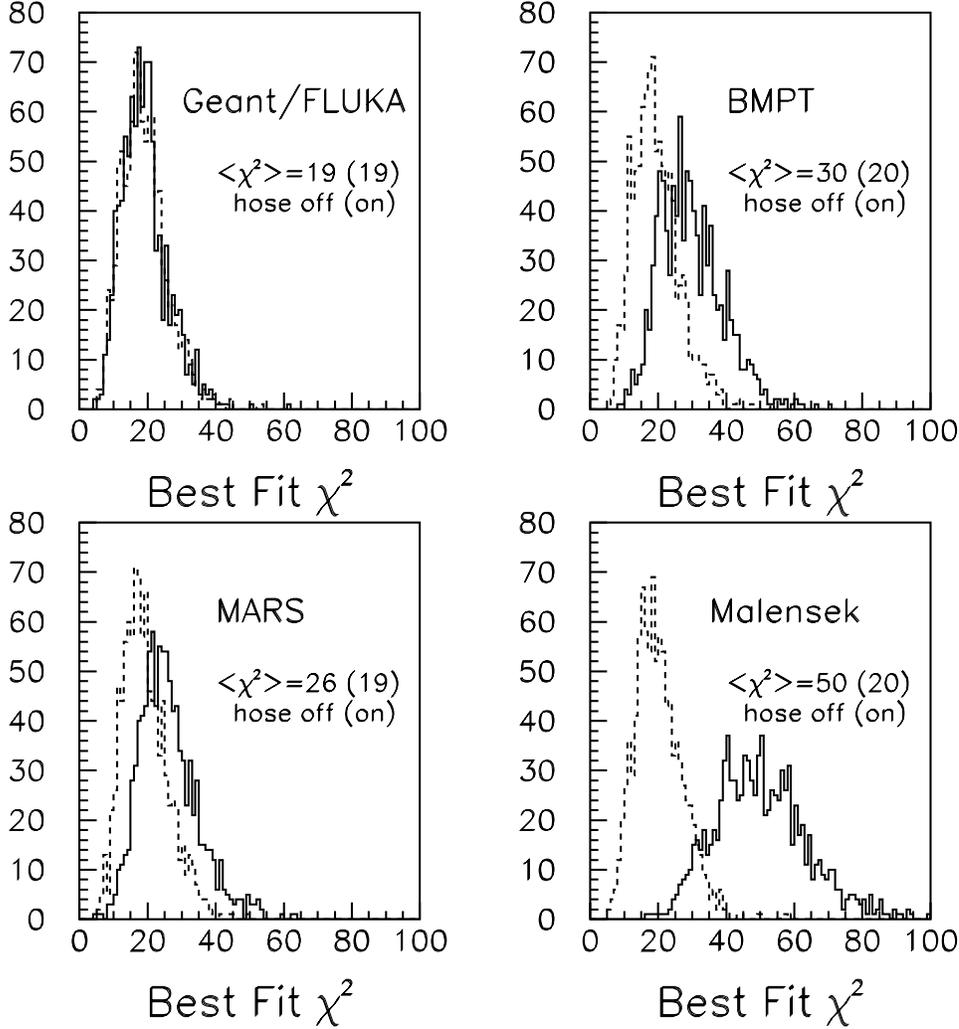


Figure 8: Simulation of 1000 MINOS experiments of 10 kt-yr. exposure in the PH2LE beam. The data were generated with $\Delta m^2 = 0.002\text{eV}^2$ and $\sin^2(2\theta) = 1.0$ and various hadron production models. The data in each Geant/FLUKA model was used to calculate \mathcal{R}_{FN} . The solid (dashed) histograms are for hose off (on).

with *no* oscillations present, generated with each of the four models, with and without hose. Figure 9 shows $\Delta\chi^2 \equiv \chi_{\text{no osc.}}^2 - \chi_{\text{best fit}}^2$, where $\chi_{\text{no osc.}}^2$ is the chi square of the fit to the no oscillations scenario, while $\chi_{\text{best fit}}^2$ is the chi square of the fit to the optimal choice of Δm^2 and $\sin^2(2\theta)$. For a “ 4σ ” significant signal, $\Delta\chi^2 = 16$. MINOS would falsely claim an oscillation signal in 3, 2, or 13% of experiments performed, depending upon which of the models (BMPT, MARS, or Malensek, respectively) one assumes for the beam distortion. As shown in Figure 9, the probability of falsely discovering oscillations is made to be $\sim 0.2 - 0.5\%$ with the addition of the hose, irrespective of model. While the effect is moderate, the hose does protect the experiment from false positive signals.

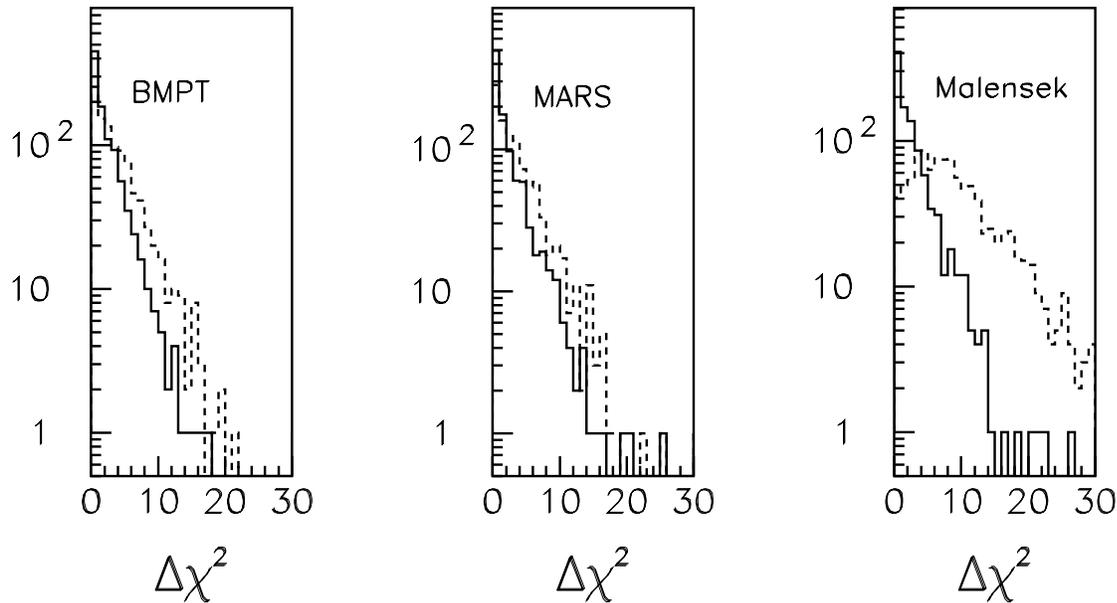


Figure 9: No-oscillation fit to 1000 MINOS experiments in the PH2LE beam. The data were generated with no oscillations and the BMPT, MARS, or Malensek models and fit to templates created using Geant/FLUKA.

4.2 If Unknown Distortions are Taken as Systematic Uncertainties

The more likely scenario is that if the Hose were not adopted as part of the NuMI design, these distortions would be incorporated as systematic uncertainties from the beam. We use the spread of the models as a measure of the systematic uncertainty from the beam. Such an increased error serves to reduce the experiment’s sensitivity.

As can be seen in Figure 10, the hose helps retain sensitivity for small signals in two ways. Here, oscillations with $\Delta m^2 = 0.001 \text{eV}^2$ and $\sin^2(2\theta) = 0.75$ were generated for 1000 MINOS experiments, each of 10 kt-yr. exposure. The upper left plot shows the fit results of experiments when no systematic uncertainty is added to the χ^2 . The upper right plot shows the fit results from 1000 experiments when systematic uncertainties are added. The lower two plots show the same systematics off/on, but with the addition of hose. In each plot, only those experiments which have a “ 4σ effect,” or “ 4σ discovery,” of oscillations are shown, hence the number of entries in each plot is significant. The hose increases likelihood of seeing a 4σ effect even with no systematic distortions, which is due to the increased event rate in the far detector with the hose on. But the fact that the hose shows less of a drop in efficiency for 4σ discovery when systematics are included indicates that the $\sim 2\%$ systematic uncertainties at low E_ν do have an effect on MINOS sensitivity. Figure 11 shows the same hose on/off comparison, but with $\sin^2(2\theta) = 1.0$ input to the simulation, which, as expected, is less sensitive to systematics.

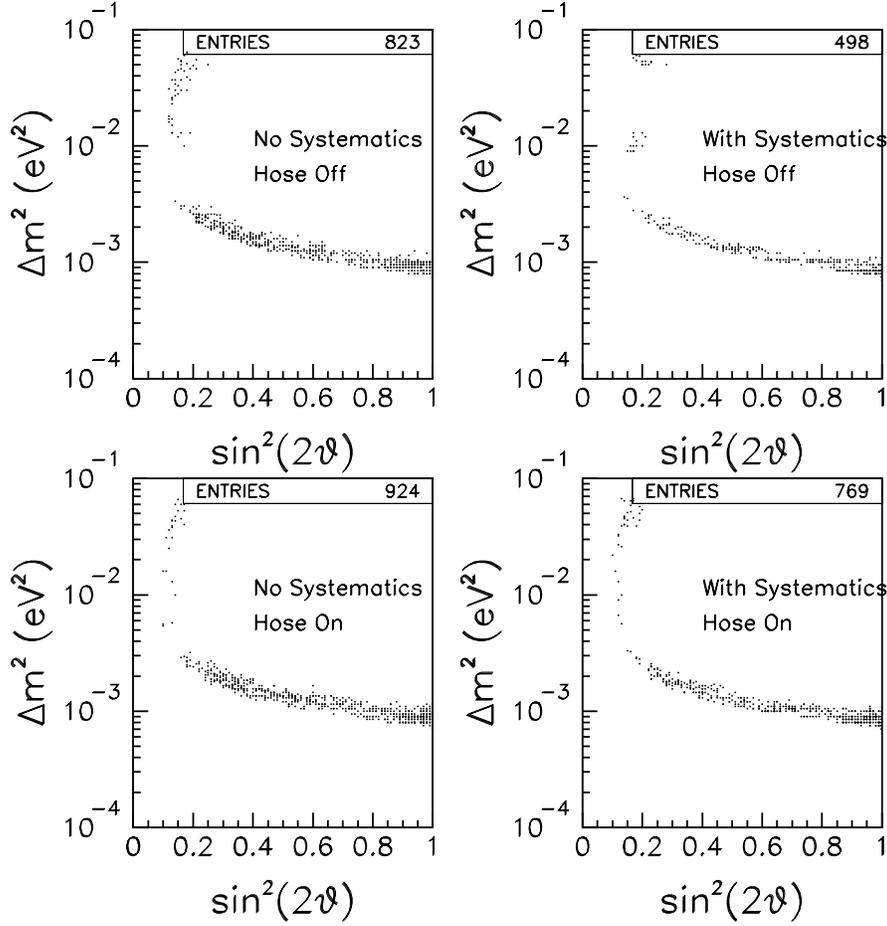


Figure 10: Simulation of 1000 MINOS experiments of 10 kt-yr. exposure in the PH2LE beam with $\Delta m^2 = 0.001 \text{ eV}^2$ and $\sin^2(2\theta) = 0.75$. Shown are central fit values from experiments which have “ 4σ ” significance.

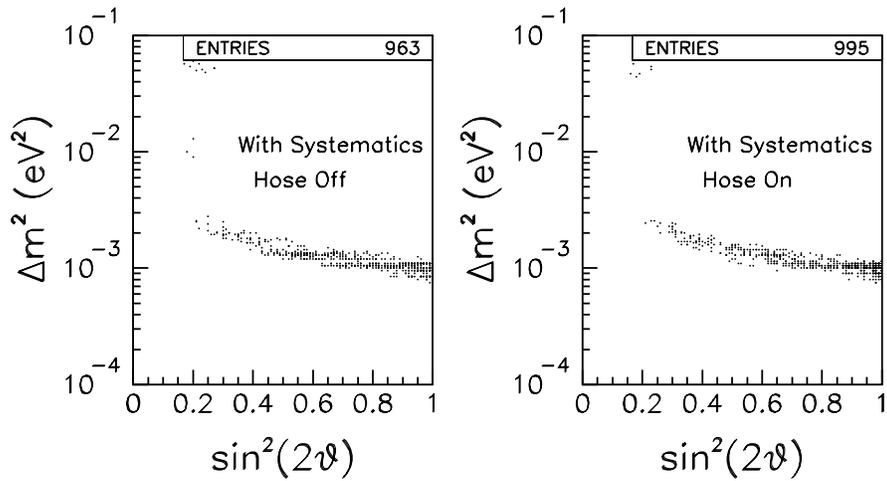


Figure 11: Simulation of 1000 MINOS experiments of 10 kt-yr. exposure in the PH2LE beam with $\Delta m^2 = 0.001 \text{ eV}^2$ and $\sin^2(2\theta) = 1.0$. Shown are central fit values from experiments which have “ 4σ ” significance.

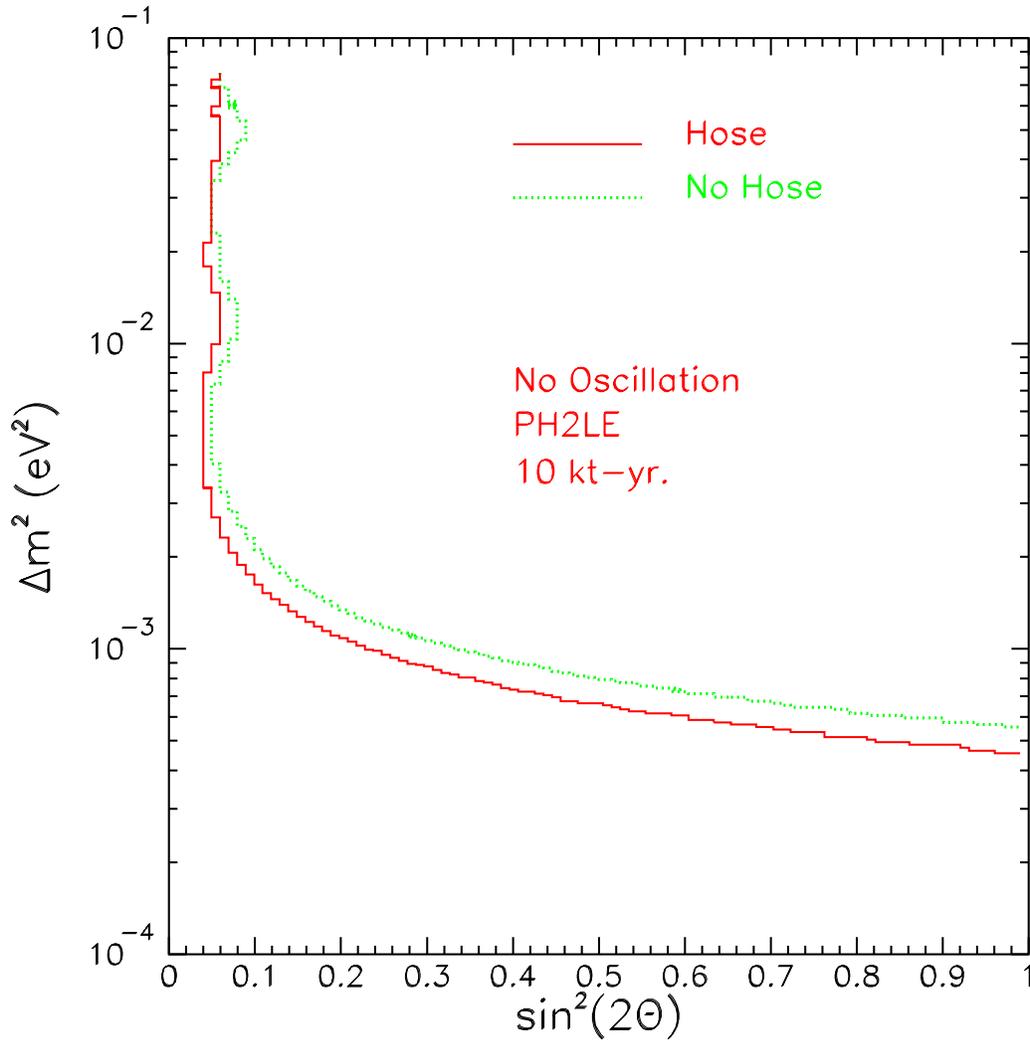


Figure 12: 90% C.L. sensitivity curves for the MINOS experiment in the PH2LE beam, with (solid curve) and without (dashed curve) the hadronic hose.

Figure 12 shows 90% confidence level interval for MINOS with and without the hose when no oscillations are present in the simulations. In these plots, the systematic errors from the hadronic production models have been included in the χ^2 . Figures 13 and 14 show the same when $\sin^2(2\theta) = 1.0$ and either $\Delta m^2 = 0.001$ or 0.002 eV^2 is input to the simulation. As shown in Figures 10 and 11, the improvement in sensitivity with the hadronic hose is a combination of the increased statistics and the smaller systematics.

We show in Figure 15 the central fit values for Δm^2 when the value of $\sin^2(2\theta) = 1.0$ and either $\Delta m^2 = 0.002$ or 0.006 eV^2 is input. We show the results of 1000 experiments in either case, both with and without the hadronic hose. Figure 16 shows the resolution determined in this way as a function of the Δm^2 input. For most of Δm^2 , the improvement in resolution comes from the increased statistics. That the hose on and hose off points display a slightly different behaviour around $\Delta m^2 \sim 0.005 - 0.008 \text{ eV}^2$ shows where the systematics are most important.

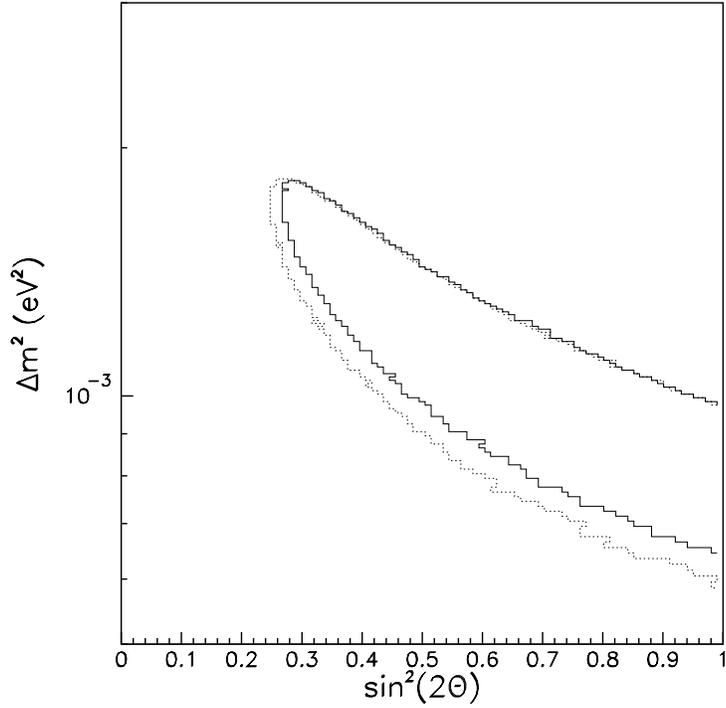


Figure 13: 90% C.L. interval for the MINOS experiment in the PH2LE beam, with (solid curve) and without (dashed curve) the hadronic hose when $\sin^2(2\theta) = 0.75$ and $\Delta m^2 = 0.001 \text{ eV}^2$ are input into the simulation.

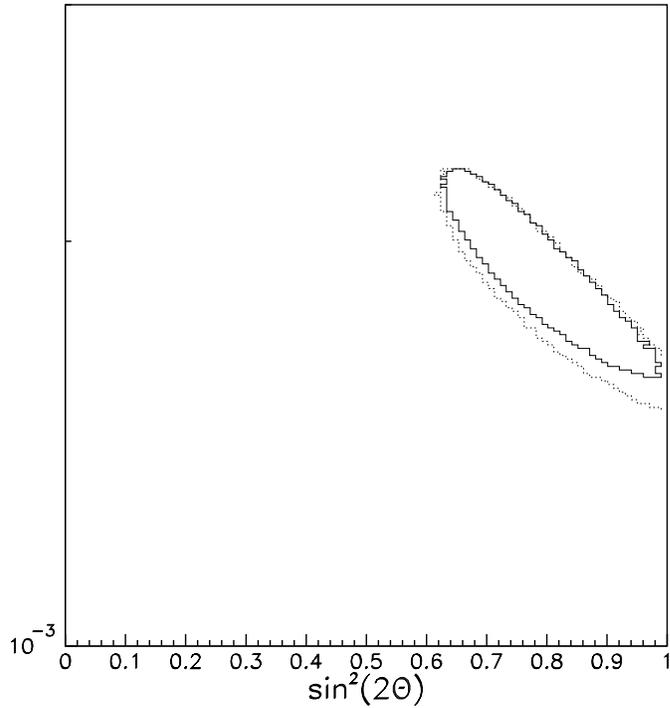


Figure 14: 90% C.L. interval for the MINOS experiment in the PH2LE beam, with (solid curve) and without (dashed curve) the hadronic hose when $\Delta m^2 = 0.002 \text{ eV}^2$ and $\sin^2(2\theta) = 0.75$ are input to the simulation.

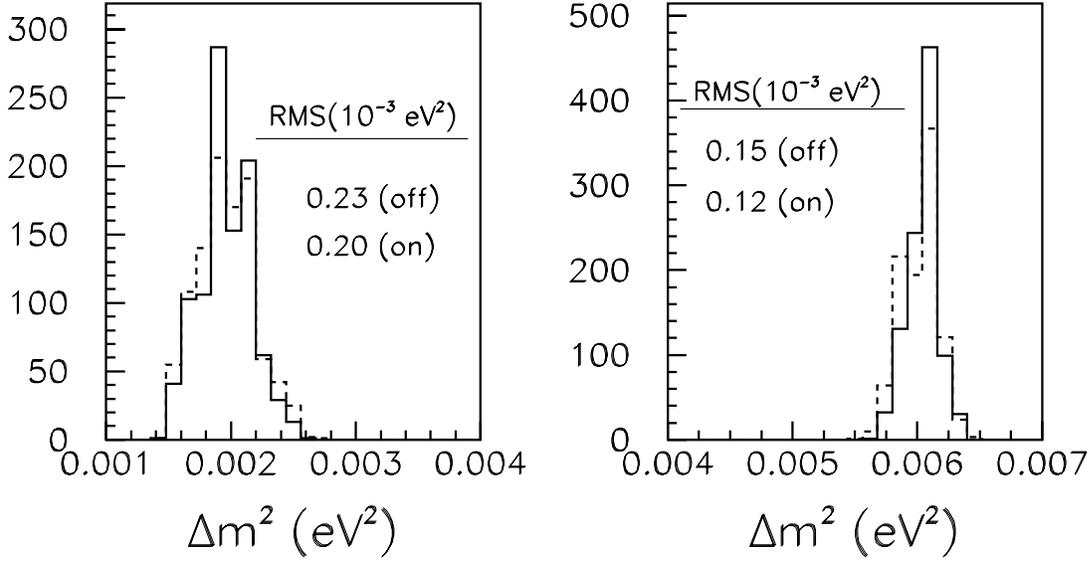


Figure 15: Simulation of 1000 MINOS experiments of 10 kt-yr. exposure in the PH2LE beam with $\Delta m^2 = 0.002$ eV² and with 0.006 eV² and $\sin^2(2\theta) = 1.0$. Shown are the fit values from the 1000 experiments, with the hose on (solid histograms) and with the hose off (dashed histograms).

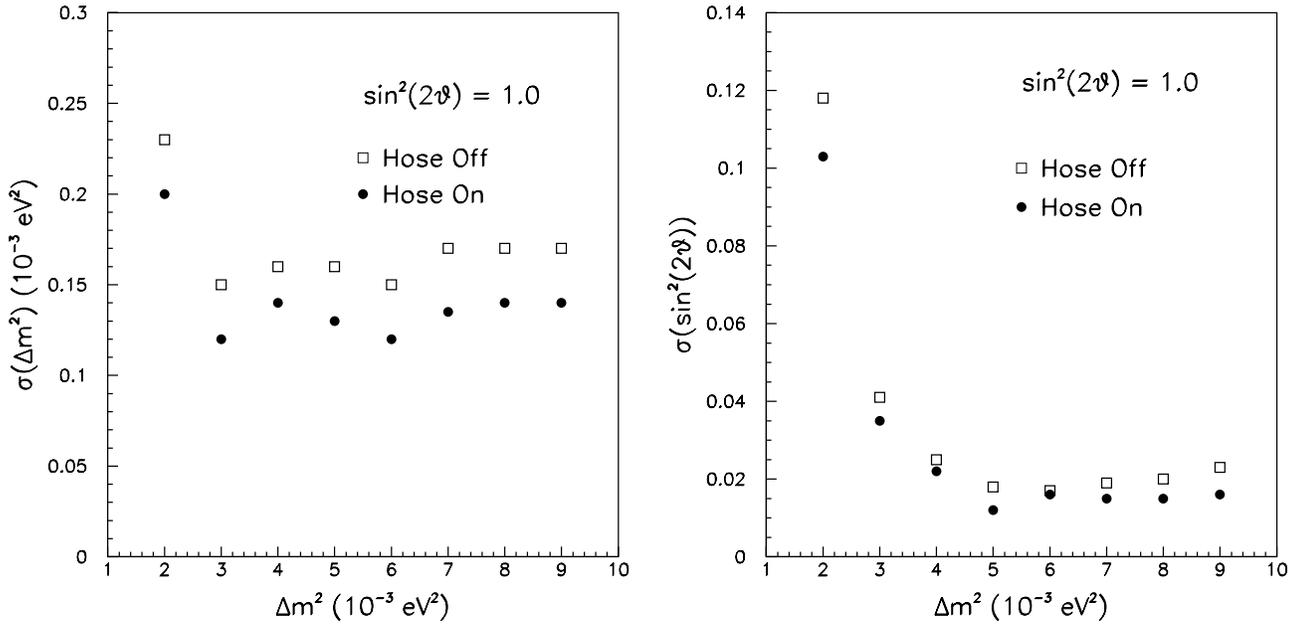


Figure 16: Resolution in Δm^2 and $\sin^2(2\theta)$ of MINOS in the PH2LE beam, with and without hose, as a function of the input Δm^2 . The resolutions are determined from the spread of 1000 experiments' central fit values.

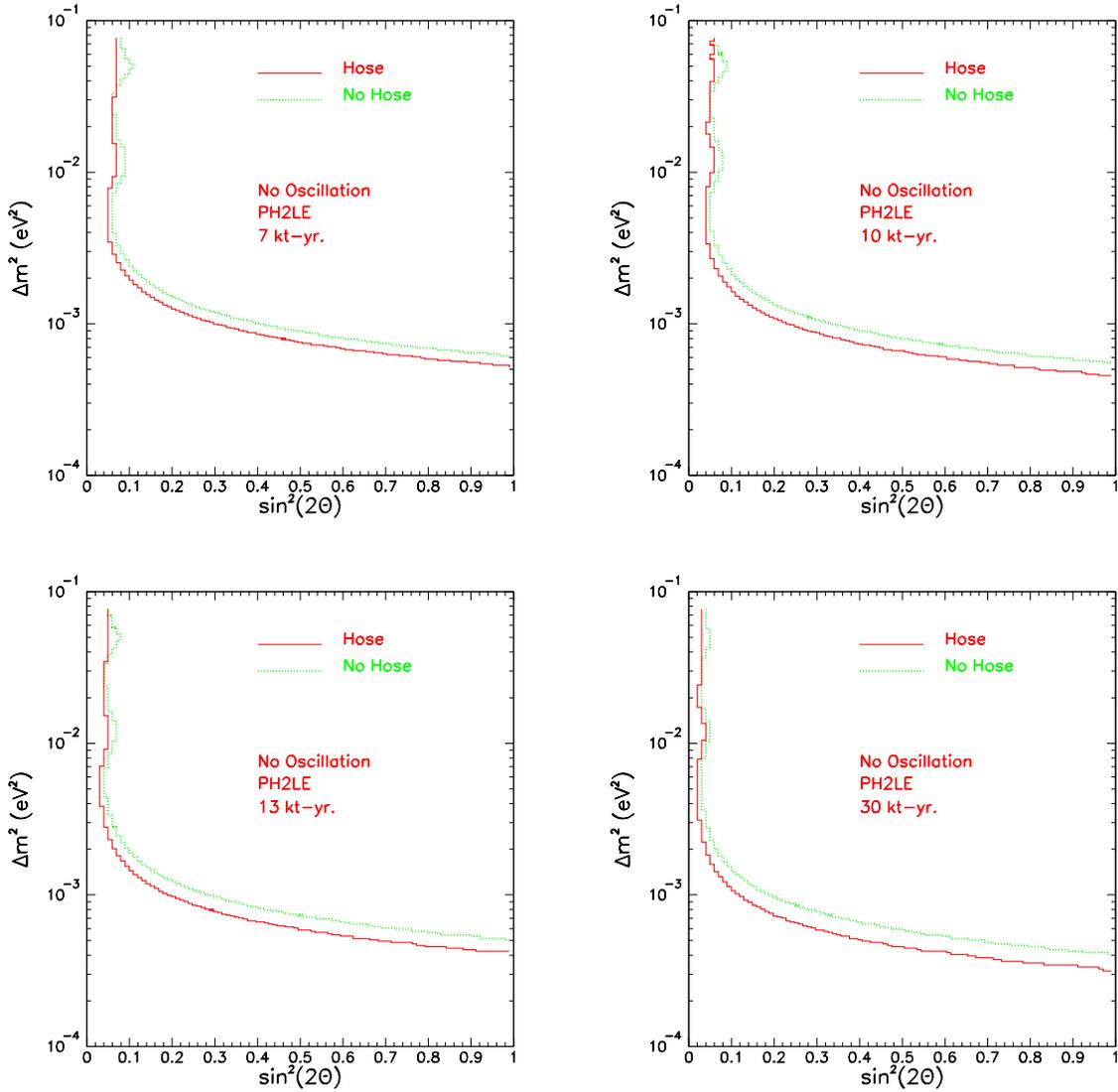


Figure 17: 90% C.L. sensitivity curves for the MINOS experiment in the PH2LE beam, with (solid curve) and without (dashed curve) the hadronic hose, generated for exposures of 7, 10, 13, and 30 kt-yr.

4.3 Statistics *vs.* Systematics

From the previous discussion it is clear that the hadronic hose plays a beneficial role in the CC disappearance measurement. The extended reach of the MINOS experiment at the very lowest Δm^2 is expected to improve as the fourth root of the statistics. Thus, the appreciable improvement shown in Figure 12 must in some way reflect on the importance of the systematic errors. As a means of demonstrating the importance of the systematics, we show in Figure 17 the expected sensitivity of the experiment for different run periods: 7, 10, 13, and 30 kt-yr (30 kt-yr. is 6 years running with the nominal MINOS far detector). In Figure 18 we show the 90% limit on Δm^2 (taken at $\sin^2(2\theta) = 1.0$) for these four exposures. As can be verified, the trend is indeed the fourth root of the exposure for both the hose on and hose off cases. However, the hose does systematically better, and a 7 kton-year exposure of taken with the hadron hose is in fact equivalent to the limit obtained in 12 kt-yrs without the hose.

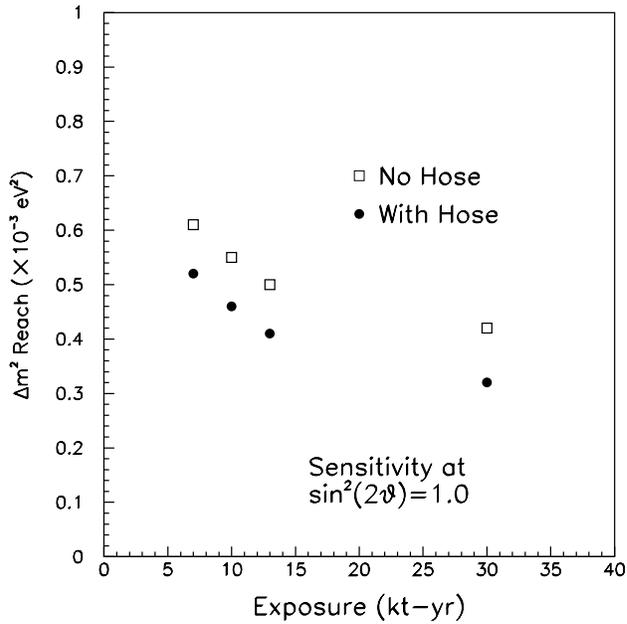


Figure 18: 90% C.L. sensitivity curves for the MINOS experiment in the PH2LE beam, with (solid curve) and without (dashed curve) the hadronic hose.

It is difficult to quantify the long-term effects of systematic uncertainties on the MINOS experiment. Sensitivity curves in the absence of oscillations do not tell the whole story. What is desired is to make the most precise measurement of the neutrino energy spectrum possible so that either precise parameter measurements can be made or the standard oscillation hypothesis confirmed. The non-standard case is addressed in the next section. One means of demonstrating 'how well we measure oscillations' is to plot the parameter resolutions as a function of running time, as shown in Figure 19. As shown in Figure 19, the slope of improvement is much slower without the hose than with the hose (in the interval 5 - 20 kt-yr.).

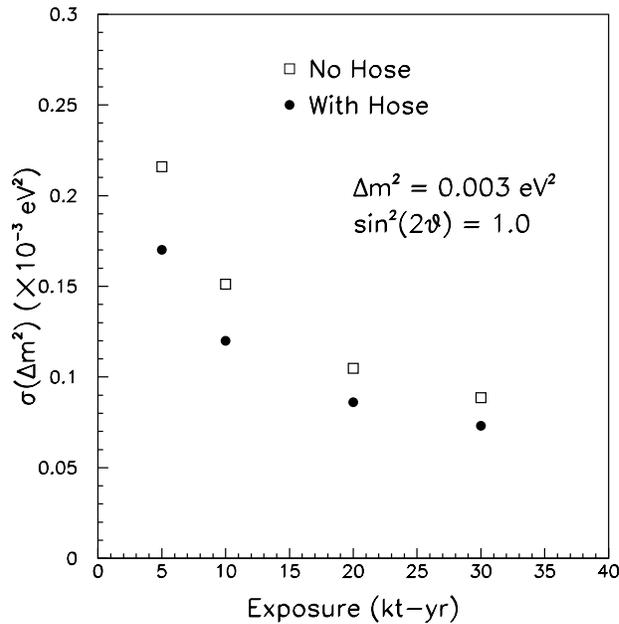


Figure 19: The resolution in the parameter Δm^2 as a function of MINOS running time, calculated assuming both no hose and with the hose. For this calculation, $\Delta m^2 = 0.003 \text{ eV}^2$ and $\sin^2(2\theta) = 1.0$ were input into the simulation.

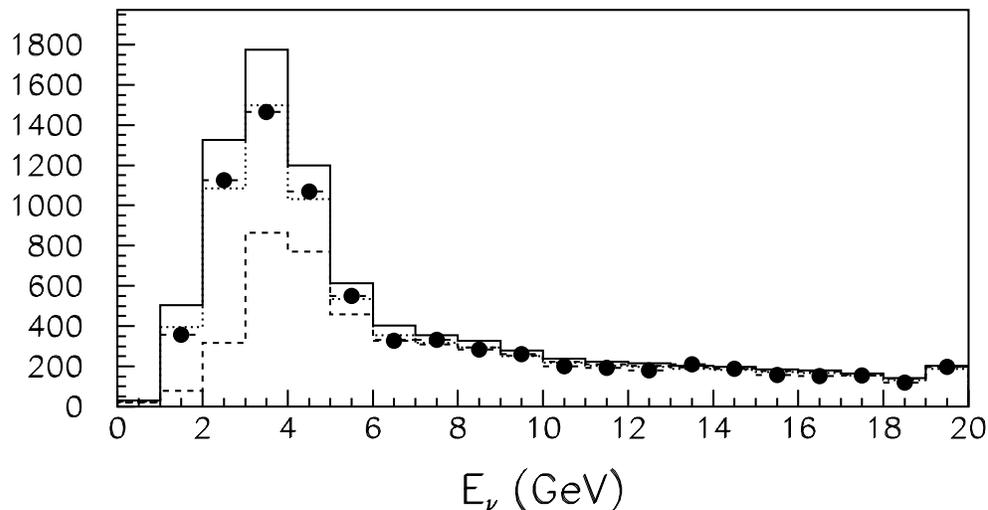


Figure 20: Simulation of MINOS experiments of 30 kt-yr. exposure in the PH2LE beam in which ν_μ depletion due to extra dimensions model of Barbieri *et al.*[9]. The solid histogram is the expectation for no oscillations, the dashed histogram is the expectation for for standard oscillations with $\Delta m^2 = 0.002 \text{ eV}^2$ and $\sin^2(2\theta) = 1.0$. The points are the far detector data.

5 Sensitivity to New Physics

As another means of demonstrating the loss of sensitivity due to such systematic uncertainties, we have investigated the experiment's sensitivity to other neutrino disappearance phenomena, such as the model of Barbieri *et al.* in which neutrinos oscillate through propagation in large extra dimensions [9] or the model of Barger *et al.*, in which neutrinos, by virtue of their non-zero mass, are allowed to decay[10]. Each of these models produces acceptable fits to the Super Kamiokande data, but MINOS may hope to discriminate among these models because of its different L/E reach from Super K. We hope eventually to investigate $\nu_\mu - \nu_s$ oscillations. Each of these models have a slightly different shape in L/E_ν than the standard $\nu_\mu - \nu_\tau$ oscillations. Ultimately, MINOS must be able to demonstrate whether the the ν_μ disappearance measurement is due to the $\sin^2(1.27\Delta m^2 L/E_\nu)$ oscillation shape or some other effect. In this study we assumed that MINOS ran for 6 years (30 kt-yr.) exposure in the PH2LE beam, so that statistical errors would not be the limiting factor for a non-standard 'discovery'.

5.1 Extra Dimensions

The neutrino energy spectrum MINOS would see in one experiment for the extra dimension model is shown in Figure 20. In the extra dimension model, standard neutrino species oscillate with Kaluza-Klein states which live in the extra dimensions [9]. In this model, the survival probability for ν_μ 's is:

$$P(\nu_\mu \rightarrow \nu_\mu) = \left| 1.0 - \text{erf} \frac{\pi \xi^2}{R} \sqrt{-i \frac{L}{2E_\nu}} \right|^2,$$

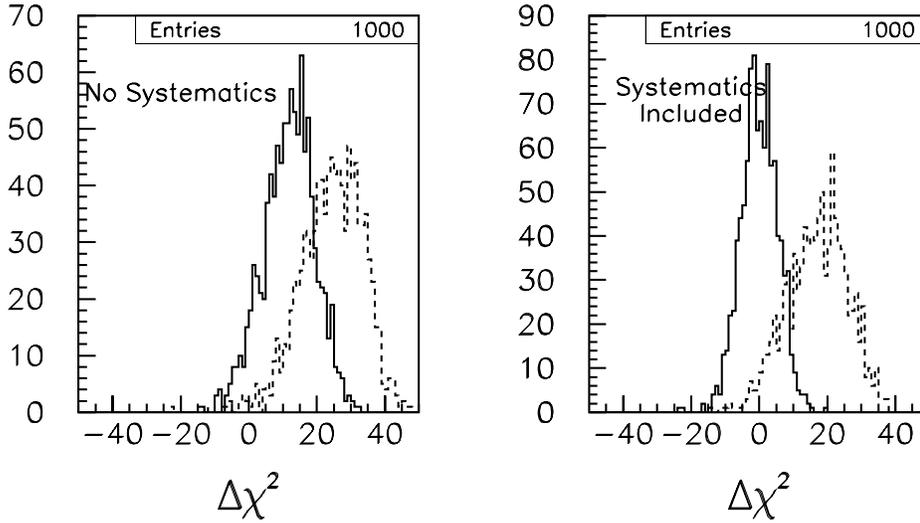


Figure 21: Simulation of 1000 MINOS experiments of 30 kt-yr. exposure in the PH2LE beam in which ν_μ depletion due to extra dimensions occurred. Shown is $\Delta\chi^2$, which is the difference in χ^2 between the best fit to the standard oscillation hypothesis and the neutrino decay hypothesis. The solid histogram is for no hose, the dashed is with the hose on.

where the parameter $\xi = mR$, m is the mass of the Kaluza Klein state and R is the largest radius of the extra dimensions. Barbieri *et al* claim that a completely acceptable fit of the Super Kamiokande data can be obtained with the parameter $\xi^2/R \sim 0.01$. MINOS could hope to distinguish between standard oscillations and these extra dimensions due to its different L/E reach and because this disappearance probability is approximately linear in (L/E_ν) , as opposed to the $(L/E_\nu)^2$ dependence of standard oscillations.

Without the hose, MINOS could rule out standard oscillations in 29.3% of experiments where extra dimensions were generated. With the hose, and with no systematic uncertainties in the χ^2 , this number jumps to 83% (see Figure 21). This jump simply is due to the increased yield of the hose at low E_ν . If systematic uncertainties are included in the χ^2 test, then MINOS could rule out standard oscillations in 0.1% (57%) of experiments with the hose off (on). That the hose on efficiency does not also drop indicates that the reduced systematics at low E_ν with the hadronic hose are important for observing this subtle shape difference.

Figure 22 shows, from 1000 MINOS experiments generated with the extra dimension model, what happens when the experiment is “confused” and falsely identifies this as a standard $\nu_\mu - \nu_\tau$ oscillation. Plotted are those experiments where standard oscillations are not excluded. Admittedly, the best fit values are in unusual regions of parameter space, so this might be a “tip-off” to the experiment to run the medium energy beam, but such a run would not show an oscillation dip and the experiment might end up with no definitive result either for oscillations or new physics.

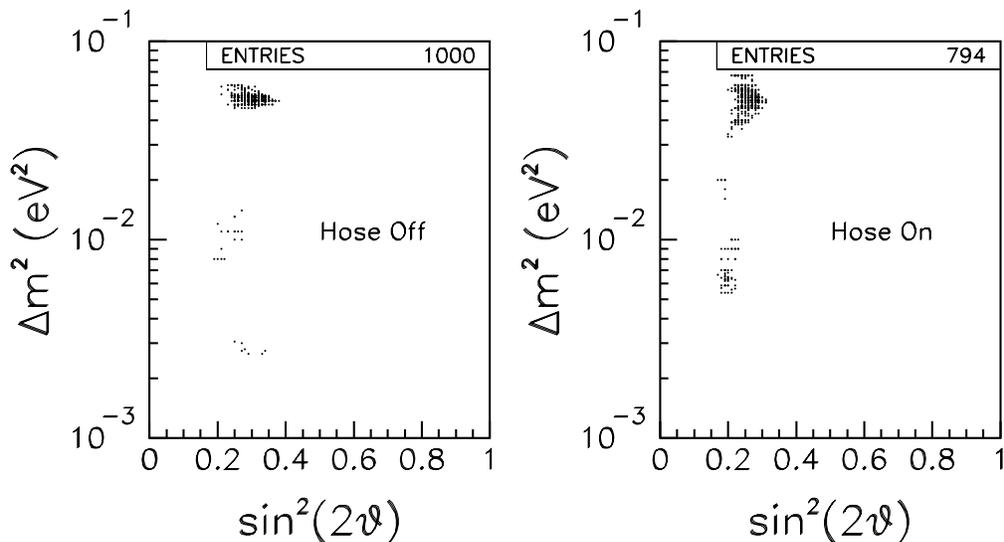


Figure 22: Simulation of 1000 MINOS experiments of 30 kt-yr. exposure in the PH2LE beam in which ν_μ depletion due to extra dimensions [9] occurred. Shown are the central fit values from experiments in which the extra dimensions were mistakenly identified as standard oscillations with 4σ C.L.

5.2 Neutrino Decay

The neutrino decay model of Barger gives a survival probability of ν_μ 's which depends upon two parameters just like standard oscillations:

$$P(\nu_\mu \rightarrow \nu_\mu) = \sin^4 \theta + \cos^4 \theta e^{-\alpha L/E} + 2 \sin^2 \theta \cos^2 \theta e^{-\alpha L/2E} \cos\left(\frac{\delta m_{23}^2 L}{2E}\right)$$

where the ν_μ state is a superposition of mass states, $\nu_\mu = \cos \theta \nu_2 + \sin \theta \nu_3$, and the ν_2 state is the one which is allowed to decay. The parameter $\alpha = m_2/\tau_2$ is the mass/lifetime ratio of the unstable state. The parameter δm_{23}^2 is the mass difference of ν_2 and ν_3 and this last term describes ν_μ disappearance due to mixing. The authors of [10] note two limiting cases for this survival probability, depending upon whether or not the ν_2 state decays to the ν_3 state or some other neutrino state ν_4 .

If the ν_2 state is allowed to decay to the ν_3 , $\nu_2 \rightarrow \nu_3 + J$ where J is some undetectable Majoron, then the ν_μ can disappear by either mixing or by decay. The authors of [10] claim that in this case the $\delta m_{23}^2 = m_2^2 - m_3^2$ is limited by K decay to be large and the survival probability's last term averages to zero. In this case the survival probability is

$$P_{\mu\mu} = \sin^4 \theta + \cos^4 \theta e^{-\alpha L/E},$$

which I've called the "large Δm^2 neutrino decay model" in Figure 23. The authors of [10] have fit this model to the Super K data, and determine best fit parameters to be $\alpha = 1/12, 800$ km/GeV, and $\sin^2 \theta = 0.03$. For these parameter choices, the survival probability is 92% at 3 GeV, the peak of the PH2LE beam. Thus, MINOS is not very

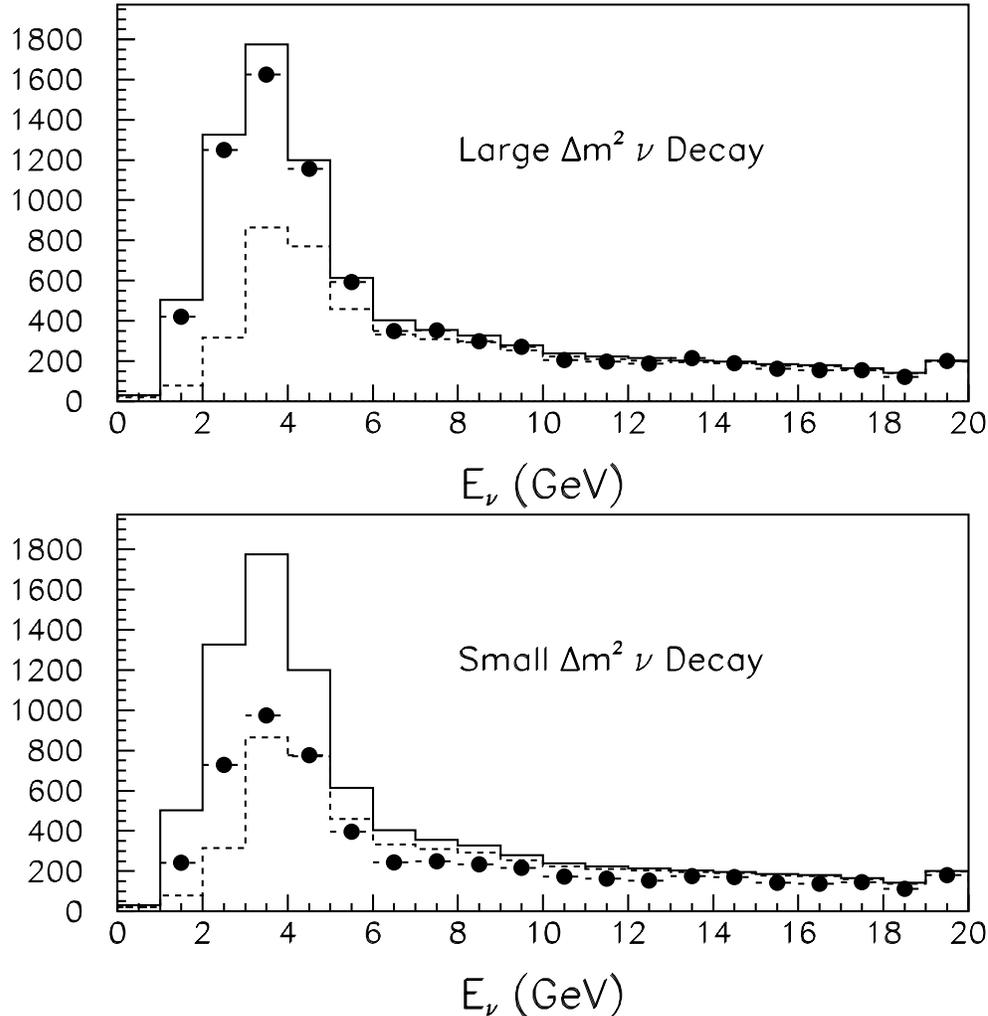


Figure 23: Simulation of MINOS experiments of 30 kt-yr. exposure in the PH2LE beam in which ν_μ depletion due to either of the two neutrino decay models of Barger *et al.*[10]. The solid histogram is the expectation for no oscillations, the dashed histogram is the expectation for for standard oscillations with $\Delta m^2 = 0.002 \text{ eV}^2$ and $\sin^2(2\theta) = 1.0$. The points are the far detector data.

sensitive to this model, and indeed we found that the χ^2 fit of such a model to standard the $\nu_\mu - \nu_\tau$ oscillations hypothesis is always acceptable, with or without the hose. The typical value for Δm^2 is found to be ~ 0.05 . Fortunately, this form of the neutrino decay model is now ruled out by the Super Kamiokande data [11].

The second, so-called “small Δm^2 ”, neutrino decay model in Figure 23 results when the ν_2 state decays to other (sterile) neutrino species ν_4 , then the δm_{23}^2 in the equation above which arises due to mixing is not limited by kaon decay data and can be quite small. If it is indeed very small the last cosine is 1.0, and

$$P(\nu_\mu \rightarrow \nu_\mu) = \left(\sin^2 \theta + \cos^2 \theta e^{-\alpha L/2E} \right)^2$$

which Barger *et al.* show fit the Super Kamiokande quite well, and is not currently excluded. Their best fit parameters are $\cos^2 \theta = 0.3$ and $1/\alpha = 63 \text{ km/GeV}$. [10] This gives a survival probability of just 0.40 at $E_\nu = 3 \text{ GeV}$, which should be quite observable in MINOS.

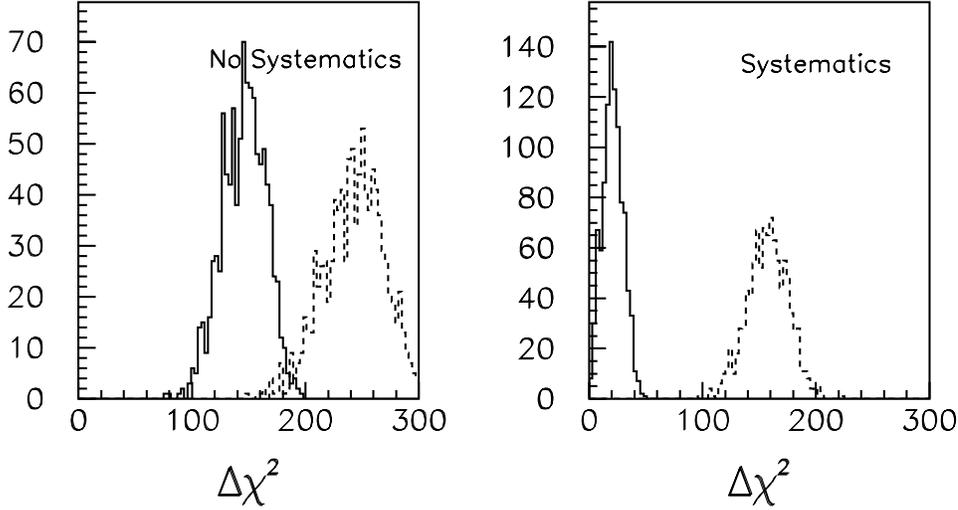


Figure 24: Simulation of 1000 MINOS experiments of 30 kt-yr. exposure in the PH2LE beam in which ν_μ depletion due to neutrino decay occurred. Shown is $\Delta\chi^2$, which is the difference in χ^2 between the best fit to the standard oscillation hypothesis and the neutrino decay hypothesis. The solid histogram is for no hose, the dashed histogram is with the hose on.

Figure 24 shows the χ^2 comparison when 1000 MINOS experiments generated with the small Δm^2 neutrino decay model are fit either to standard oscillations or to the neutrino decay hypothesis. As can be seen, the systematic uncertainties from hadron production models decrease the separation power between the two hypotheses. Here it is clear that the increased yield of the hose is not what provides the discrimination because the depletion is larger. Rather, the hose helps us exclusively because the better shape prediction in the E_ν spectrum prevents us from confusing this model with large Δm^2 standard oscillations.

6 Impact of Hadronic Hose on Searches for $\nu_\mu \rightarrow \nu_e$

The search for evidence for oscillations of muon neutrinos to electron neutrinos is one of the most important measurements MINOS will make. This section presents an estimate of the impact of the hadronic hose on this measurement.

The addition of the hadronic hose has both the potential to help and hurt the search for oscillations of $\nu_\mu \rightarrow \nu_e$. While the flux increase enhances any expected signal, backgrounds are also increased.

The search of electron-neutrino appearance has four sources of backgrounds. Two of these are hadronic showers from neutral-current interactions and high-y (low muon momentum) ν_μ charged-current interactions. Due to the missing energy carried by the out-going neutrino, neutral-current interactions are typically reconstructed as low energy showers and populate the lowest energy bins. The second two backgrounds are electro-magnetic showers from ν_e intrinsic to the beam, and ν_τ interactions (followed by $\tau \rightarrow e$ decay) from oscillations of $\nu_\mu \rightarrow \nu_\tau$.

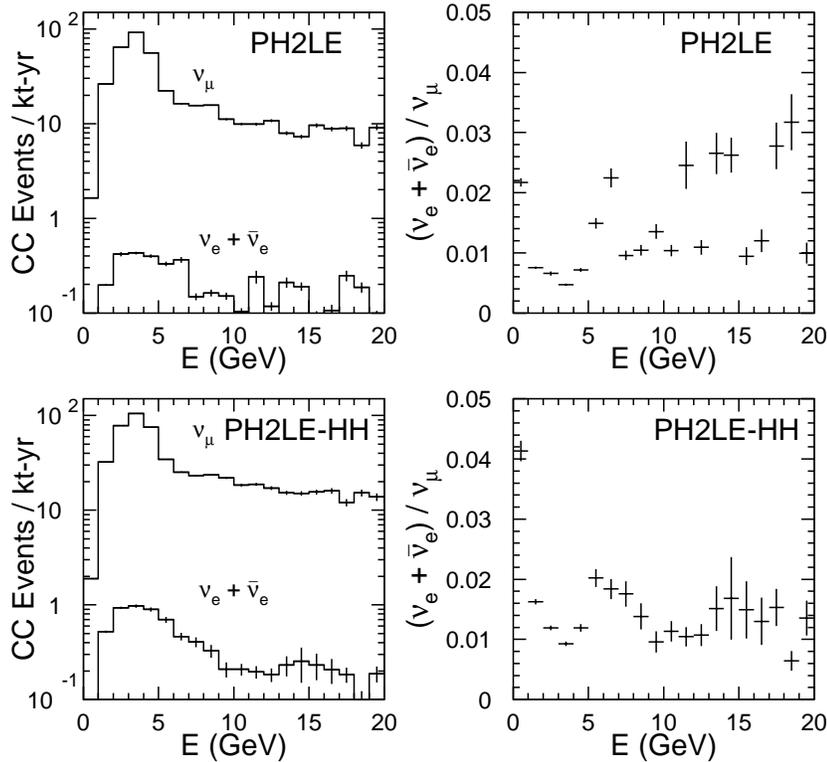


Figure 25: Expected ν_μ and ν_e event rates for the PH2LE (top) and PH2LE-HH beams (bottom).

The hadronic hose focuses muons in addition to pions resulting in an increase of the ν_e flux in the NuMI beams. The expected ν_e event rates are plotted in Figure 25 for the low-energy beam (PH2LE) and the low-energy beam with hadronic hose (PH2LE-HH). The addition of the hadronic hose increases the ν_e rates by roughly a factor of two. Also, the hadronic hose increases the flux in the high-energy tail ($E > 6$ GeV) of the PH2LE beam by a larger factor than it increases the flux in the peak of the beam (roughly 1.5 vs. 1.3). This has the potential to increase the neutral-current component of the electron appearance signature.

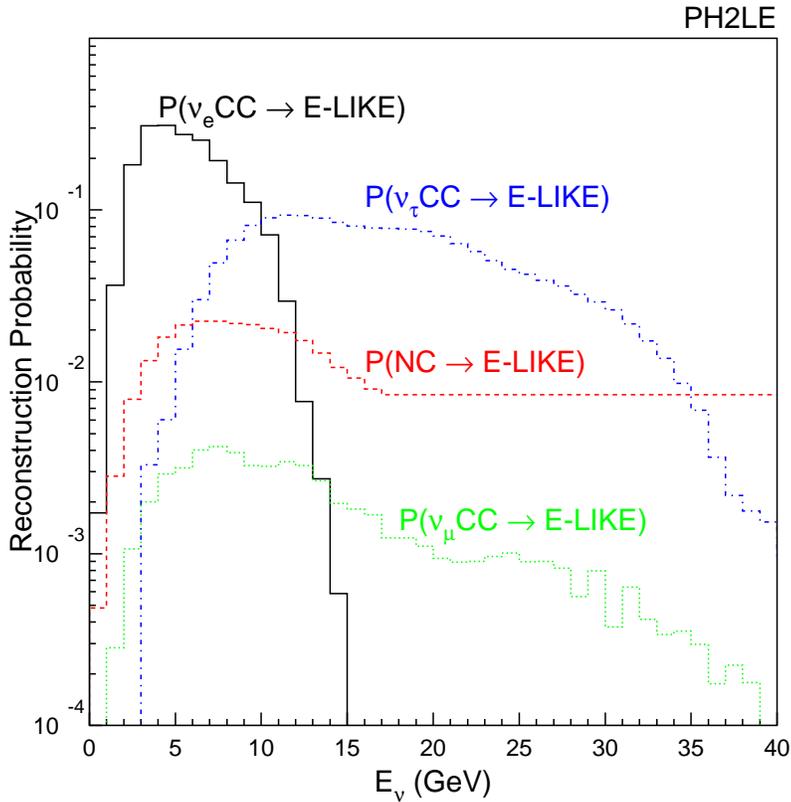


Figure 26: Reconstruction efficiencies used for the $\nu_\mu \rightarrow \nu_e$ analysis as a function of true neutrino energy.

The analysis presented here used flux inputs from simulations of the PH2LE and PH2LE-HH beams and with and without hadronic hose. Neutrino interactions on iron were simulated using the NEUGEN generator. The detector response was not simulated in detail; the effects of event reconstruction were applied at the vector level using parameterizations of the reconstruction efficiencies and energy resolutions. The reconstruction efficiencies were modeled after Ref. [12] and are shown in Figure 26. The energy resolutions were taken to be $55\%/\sqrt{E}$ for hadronic energy and $23\%/\sqrt{E}$ for the muon. Event rates were calculated assuming a

10 kt-yr exposure.

Neutrino oscillations were modeled assuming maximal $\nu_\mu - \nu_\tau$ mixing ($\theta_{23} = \pi/4$) and one mass scale dominance ($\Delta m_{12}^2 \ll \Delta m_{23}^2 \equiv \Delta m^2$). The effects of matter on neutrino propagation to the far detector alter the oscillation probabilities by as much as $\pm 20\%$ depending on the sign of Δm^2 . However, to simplify the comparison matter effects been neglected. The oscillation probabilities are then:

$$\begin{aligned}
 P(\nu_e \rightarrow \nu_\mu) &= \sin^2 2\theta_{13} \sin^2 \theta_{23} \sin^2(1.27\Delta m^2 L/E), \\
 P(\nu_\mu \rightarrow \nu_\tau) &= \cos^4 \theta_{13} \sin^2 2\theta_{23} \sin^2(1.27\Delta m^2 L/E), \\
 P(\nu_e \rightarrow \nu_\tau) &= \sin^2 2\theta_{13} \cos^2 \theta_{23} \sin^2(1.27\Delta m^2 L/E).
 \end{aligned}
 \tag{2}$$

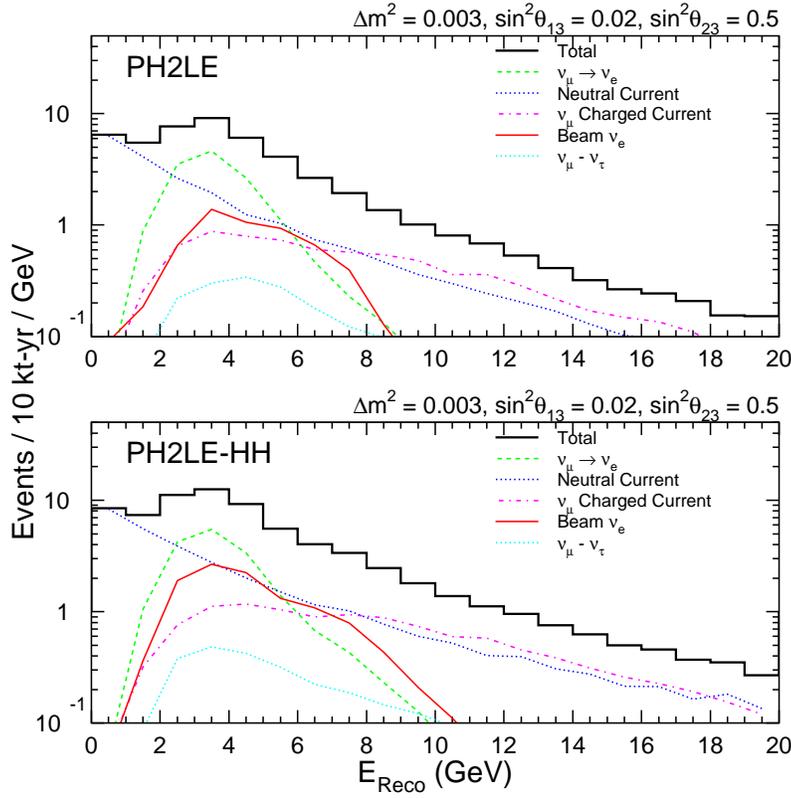


Figure 27: The expected signal and backgrounds for the $\nu_\mu - \nu_e$ oscillation search using the PH2LE beam (top) and PH2LE-HH beam (bottom).

Using these oscillation probabilities, the efficiencies and resolutions given above, spectra similar to those shown in Figure 27 were obtained for each $\sin^2 \theta_{13}$ and Δm^2 . The significance of any excess over background was computed using a χ^2 comparison to the expected background distribution. The backgrounds were assumed to be perfectly measured by the near MINOS detector.

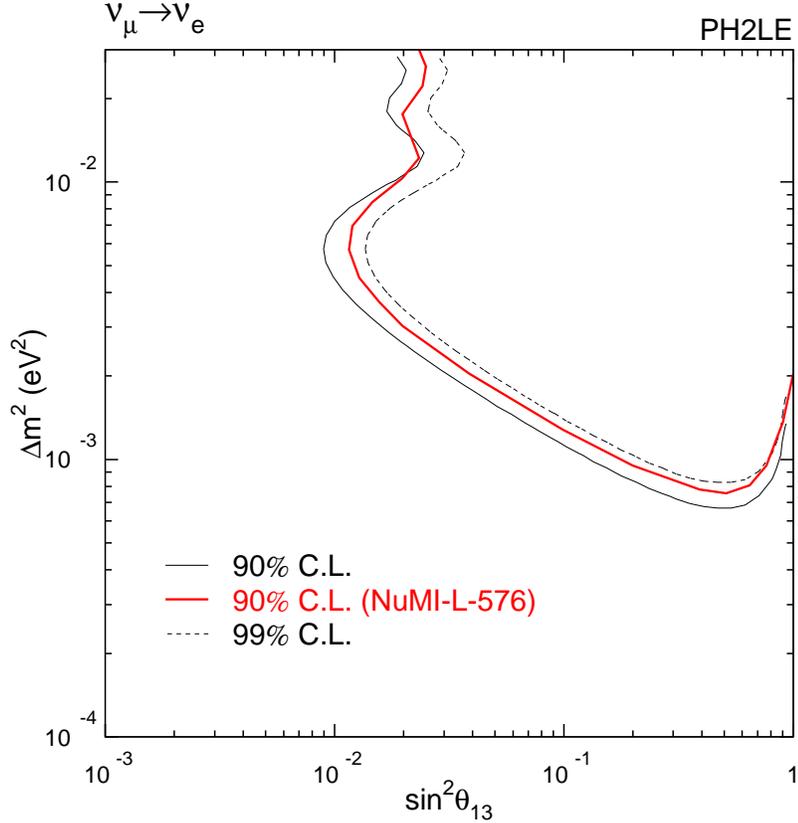


Figure 28: 90% sensitivities for PH2LE. Results from this analysis are compared with those from NuMI-L-576.

As a cross-check of the present analysis, an attempt was made to duplicate the results of Ref. [12]. The results are compared in Figure 28 and are quite similar. For the purposes of comparison, this limit curve was computed following the χ^2 definition in Ref. [12]. However, since the number of events per bin is small (< 20) the remainder of the limit curves use the χ^2 formula derived from the Poisson likelihood:

$$\chi^2 = \sum_i [2(N_i^{\text{th}} - N_i^{\text{obs}}) + 2N_i^{\text{obs}} \log(N_i^{\text{obs}}/N_i^{\text{th}})]. \quad (3)$$

The 90% limit curves are compared for the PH2LE and PH2LE-HH beams in Figure 29. The addition of the hadronic hose causes no appreciable decrease in sensitivity; the net results of the increased signal and increased background cancel. This cancellation is demonstrated in Figure 30 which shows the expected spectra at a single point in oscillation parameter space. The χ^2 comparison differs by only 0.1 out of 6.6 for 2 degrees of freedom.

As understanding of the MINOS detector increases, it is very likely that the reconstruction efficiencies used in the analysis above will improve. In this case, the increase of the beam ν_e component may become more important. To estimate the largest effect the increase in the

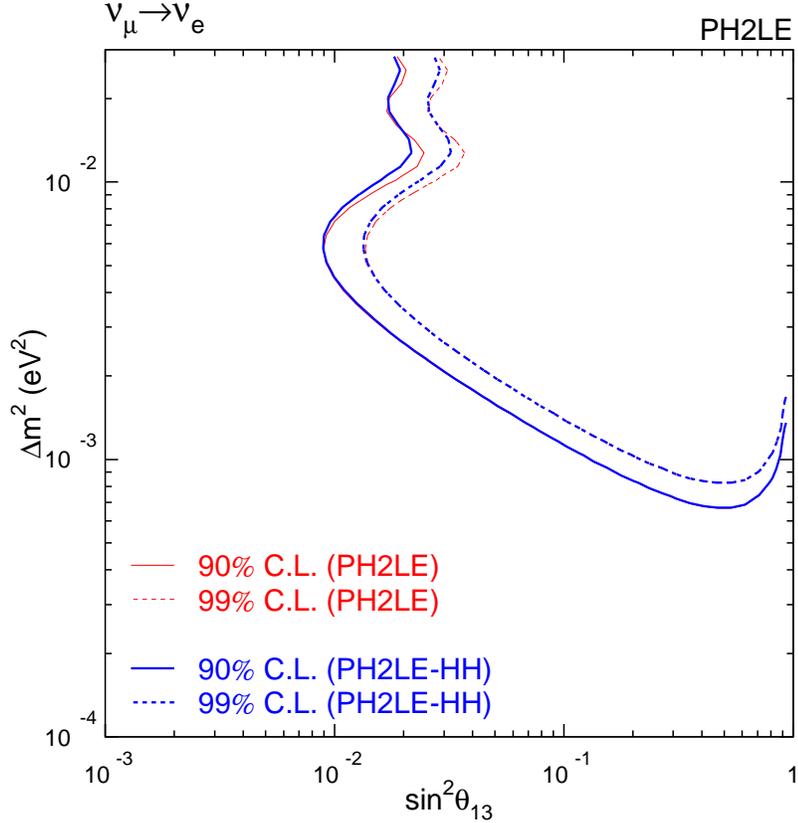


Figure 29: 90% sensitivities for PH2LE and PH2LE-HH beams. The curves only differ significantly above $6 \times 10^{-3} \text{ eV}^2$ where the PH2LE-HH is slightly more sensitive to oscillations.

beam ν_e fraction could have, the analysis above was performed assuming perfect separation of ν_e events from all other classes of backgrounds leaving the ν_e from the beam as the sole source of background. The resulting sensitivities are shown in Figure 31. The additional ν_e component of the PH2LE-HH beam results in about a 10% decrease in sensitivity. At $\Delta m^2 = 0.003 \text{ eV}^2$, the minimum allowed $\sin^2 \theta_{13}$ increases from 3.5×10^{-3} to 3.0×10^{-3} (15%); at $\sin^2 \theta_{13} = 0.5$ the minimum allowed Δm^2 increases from 2.6×10^{-4} to $2.7 \times 10^{-4} \text{ eV}^2$ (4%).

As a final study, we investigated what would the contours look like for a ν_e signal. Oscillations were generated with $\Delta m^2 = 0.0035 \text{ eV}^2$ and $U_{e3}^2 = 0.05$ (close to the CHOOZ limit), and for $U_{e3}^2 = 0.01$, taking $\theta_{23} = \pi/4$. The confidence level intervals for the two cases are shown in Figures 32 and 33, respectively. As can be seen, the allowed regions are nearly identical for the hose on or hose off cases, with the hose providing a slightly tighter bound at large $\sin^2 \theta_{12}$: for the $U_{e3}^2 = 0.05$ case, for example, the 90% C.L. allowed regions are 0.031-0.074 with no hose, and 0.031-0.073 with the hose. For the $U_{e3}^2 = 0.01$ case, the 90% C.L. allowed regions are 0.0-0.026 with no hose, and 0.0-0.025 with the hose. Thus, the

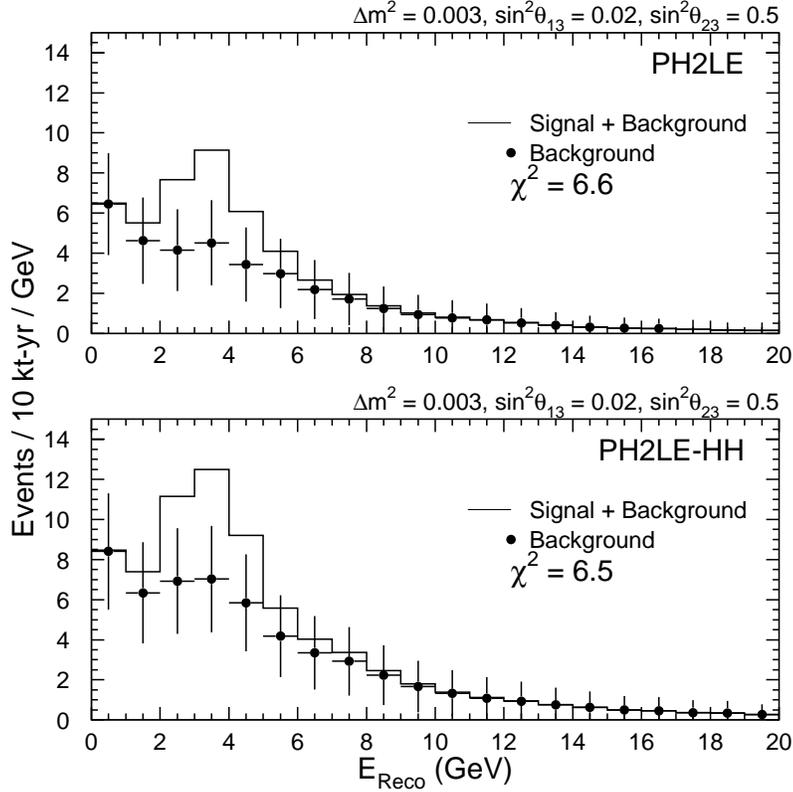


Figure 30: Comparison of the expected signal and backgrounds for the PH2LE (top) and PH2LE-HH (bottom) beam at $\Delta m^2 = 0.003 \text{ eV}^2$, $\sin^2 \theta_{13} = 0.02$, and $\sin^2 \theta_{23} = 0.5$. The significance of signal over backgrounds is very similar in the two cases.

hose does not have a significant impact on the parameter resolutions in the case of an actual signal observed in MINOS.

References

- [1] J. Hylen *et al.*, “Proposal to Include Hadronic Hose in the NuMI Beamline,” Fermilab NuMI-B-542, Oct. 1999.
- [2] J. Hylen *et al.*, “Technical Design Report for the Hadronic Hose”, NuMI-B-610 (2000).
- [3] Mark Messier *et al.*, forthcoming NuMI-B note.
- [4] *GEANT Detector Description and Simulation Tool*, CERN Program Library, W5013 (1994).

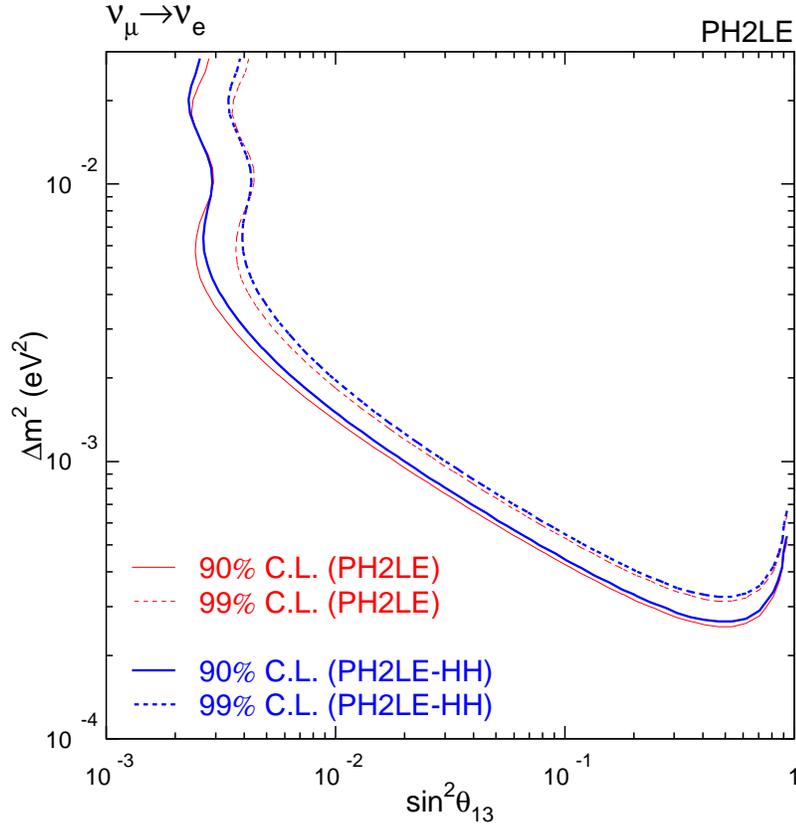


Figure 31: 90% sensitivities for PH2LE. Results are compared for the PH2LE and PH2LE-HH beams using perfect reconstruction efficiencies.

- [5] M. Bonesini, A. Marchionni, F. Pietropaolo, and T. Tabarelli de Fatis, “Empirical Fits to Particle Production in Nuclear Targets”, talk given at CERN Experimental Particle Physics Seminar, April, 2000 (unpublished).
- [6] N.V. Mokhov, “The MARS Monte Carlo”, Fermilab FN-628 (1995); O.E. Krivosheev *et al.*, Proc. of the Third and Fourth Workshops on Simulating Accelerator Radiation Environments (SARE3 and SARE4), Fermilab-Conf-98/043(1998) and Fermilab-Conf-98/379(1998).
- [7] A.J. Malensek, “Empirical Formula for Thick Target Particle Production,” Fermilab FN-341, Oct. 1981.
- [8] D. A. Petyt, NuMI-L-481, “Low Δm^2 Sensitivity of the T-Test,” April, 1999.
- [9] R. Barbieri, P. Creminelli, A. Strumia, hep-ph/0002199
- [10] V. Barger *et al.*, hep-ph/9907421, Phys. Rev. Lett. **82**, 2640 (1999).

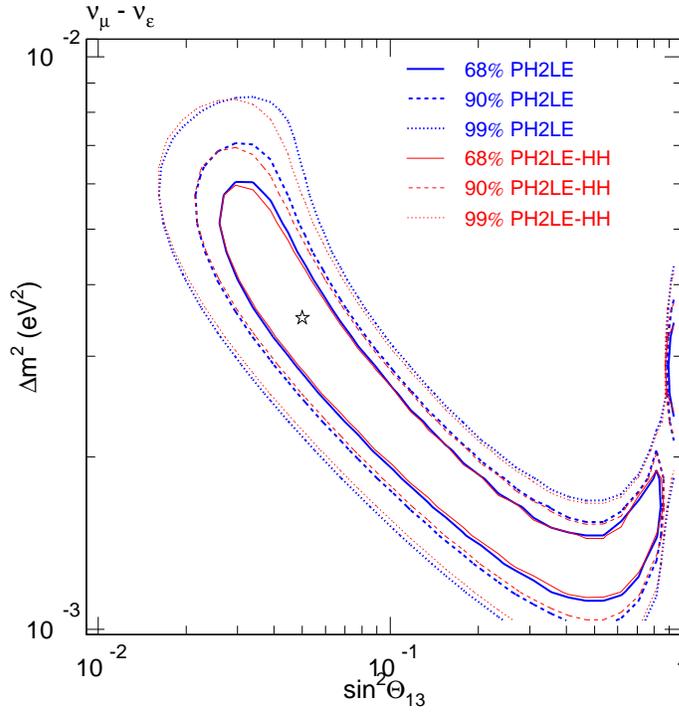


Figure 32: Allowed regions for $\nu_\mu - \nu_e$ oscillations generated with and without the hadronic hose. Shown are the allowed regions when $\Delta m^2 = 0.0035 \text{ eV}^2$ and $U_{e3}^2 = 0.05$ is input to the simulations. The hose has a small improvement at large $\sin^2 \theta_{12}$.

[11] M. Messier, “Evidence for Neutrino Mass from Observations of Atmospheric Neutrinos with Super-Kamiokande,” PhD Thesis, Boston University, 1999.

[12] D. Petyt, “ $\nu_\mu \rightarrow \nu_e$ in MINOS”, **NuMI-L-576** (Dec. 1999).

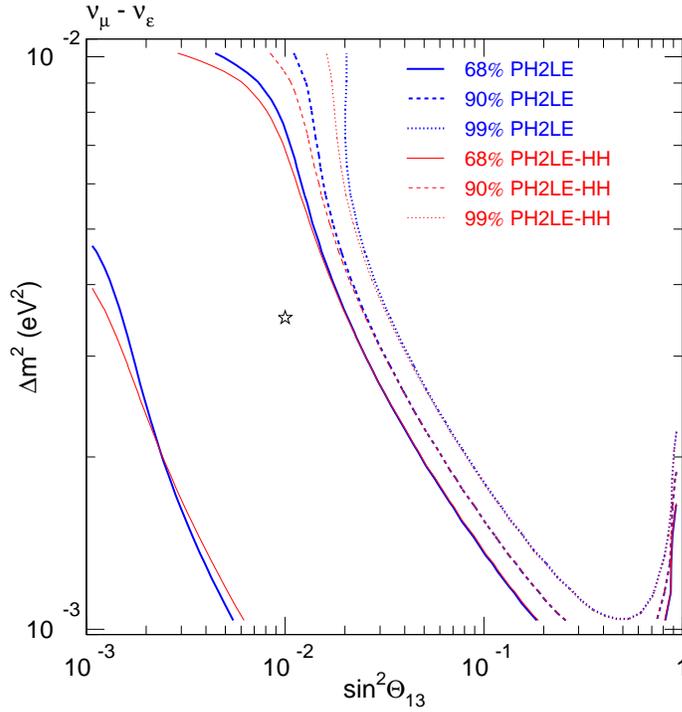


Figure 33: Allowed regions for $\nu_\mu - \nu_e$ oscillations generated with and without the hadronic hose. Shown are the allowed regions when $\Delta m^2 = 0.0035 \text{ eV}^2$ and $U_{e3}^2 = 0.01$ is input to the simulations. The hose has a small improvement at large $\sin^2 \theta_{12}$